Finite volume effects for nucleon and heavy meson masses

Gilberto Colangelo[a], Andreas Fuhrer[b] and Stefan Lanz[a,c]

[a] Albert Einstein Center for Fundamental Physics

Institut für Theoretische Physik, Universität Bern

Sidlerstr. 5, CH-3012 Bern, Switzerland

[b] Department of Physics, University of California at San Diego,

9500 Gilman Drive, La Jolla, CA 92093, USA

[c] Department of Astronomy and Theoretical Physics, Lund University

Sölvegatan 14A, S 223 62 Lund, Sweden

May 11, 2010

Abstract

We apply the resummed version of the Lüscher formula to analyze finite volume corrections to the mass of the nucleon and of heavy mesons. We show that by applying the subthreshold expansion of the scattering amplitudes one can express the finite volume corrections in terms of only a few physical observables and the size of the box. In the case of the nucleon, the available information about the quark mass dependence of these physical quantities is discussed and used to assess the finite volume corrections to the nucleon mass as a function of the quark mass including a detailed analysis of the remaining uncertainties. For heavy mesons, the Lüscher formula is derived both fully relativistically and in a nonrelativistic approximation and a first attempt at a numerical analysis is made.

Contents

1 Introduction

Lattice calculations have recently almost reached physical pion masses (see e.g. Refs. [1, 2]), thereby establishing firm contact with chiral perturbation theory (ChPT) [3–5]. The effective theory therefore becomes increasingly useful to address systematic effects in lattice calculations like the finite volume, for example. To use the effective chiral Lagrangian to evaluate such effects was first advocated in Refs. [6, 7] where it was also shown that in the p-regime, where the Compton wavelength of the pion is much smaller than the size of the box, the infinite volume Lagrangian can be used for doing calculations. An alternative approach to evaluate finite volume corrections (FVC) to masses in the p-regime is the Lüscher formula [8, 9]. This relates the FVC of a particle P to an integral over the forward scattering amplitude of the same particle P off the lightest particle in the spectrum. The main contributions to this integral come from the low-energy region, while high-energy contributions are exponentially suppressed. This justifies the use of amplitudes evaluated in ChPT as an input. An improved version of the Lüscher formula, where subleading terms are resummed, was already successfully applied to meson masses and, in a generalized form, to coupling constants [10–13]. FVC for the nucleon mass in ChPT and the Lüscher formula have been discussed in [14–16].

One of the advantages of the Lüscher formula is that it allows a relatively easy estimate of higher order effects and yields simple analytical expressions. In Ref. [12] it was shown that inserting the tree level $\pi\pi$ scattering amplitude into the resummed Lüscher formula exactly reproduces the one-loop result of the FVC for the pion mass evaluated in ChPT. At the two-loop level, this does not hold anymore, because in the derivation of the Lüscher formula, only one propagator is considered to be in finite volume — two-loop contributions in which propagators appearing in different loops are simultaneously taken in finite volume are exponentially subdominant and neglected from the start in Lüscher's approach. However, the two-loop FVC of the pion mass were explicitly calculated and compared with the result of the resummed Lüscher formula with a one-loop amplitude in the integrand in Ref. [17]. It was found that the difference is very small and thereby a solid argument was provided to base further analyses of FVC on the resummed Lüscher formula.

In this paper we apply the latter to estimate the FVC to masses of heavy particles, and in particular to nucleons and to mesons containing a heavy quark. Although these two kind of particles are very different — nucleons are spin-1/2 particles and are much lighter than the spin-0 B mesons, for example — the essential common feature is that both are much heavier than the pions. Neither the exact value of their mass, nor their spin, make a qualitative
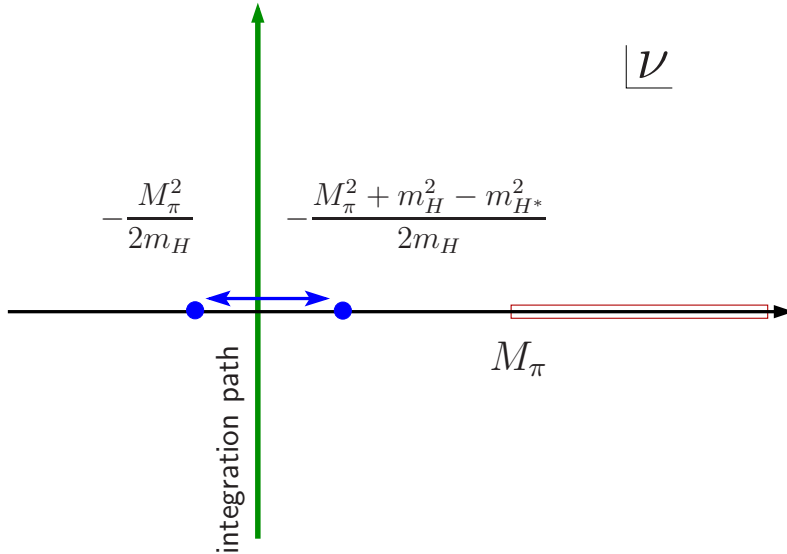
2

Figure 1: Singularities of the forward scattering amplitude in the complex ν-plane. The cut on the real axis is due to the intermediate state $H\pi$ and the pole on the left-hand side of the imaginary axis to the intermediate H^* state (or H in the case of the nucleon). The position of the pole depends on $m_{H^*}^2 - m_H^2$ and moves to the right-hand side of the imaginary axis if $m_{H^*}^2 - m_H^2 > M_\pi^2$. Notice that the amplitude is an even function of ν and that for clarity we have drawn only half of the singularities.

difference in the evaluation of the FVC. What makes the treatment of the two cases very similar is that the singularity structure of the πH scattering amplitude at low energy (H being the heavy particle) is dominated by a single pole due to the exchange of a particle degenerate (or almost degenerate) with H. The forward scattering amplitude is a function of only one kinematical variable ν. The pole due to the exchange of a particle H^* in the s-channel is located at

$$\nu = -(M_\pi^2 - m_{H^*}^2 + m_H^2)/(2m_H) \stackrel{m_{H^*} \to m_H}{\longrightarrow} -M_\pi^2/(2m_H) \,, \qquad (1)$$

as illustrated in Fig. 1. If $m_{H^*}^2 - m_H^2 > M_\pi^2$ the pole is on the right-hand side of the integration path (which coincides with the imaginary axis) and the Lüscher formula contains only the term with the integral. As we take the limit $m_{H^*} \to m_H$ the pole moves to the left until it crosses the imaginary axis and finally reaches $\nu = -M_\pi^2/(2m_H)$. When the pole crosses the imaginary axis an extra local contribution to the Lüscher formula appears [8], which is exponentially leading. The study of the heavy meson case, in which we

can vary $\Delta_* \equiv m_{H^*} - m_H$ and even send it to zero, allows us to better understand the role of the local, exponentially leading contribution in the Lüscher formula. We stress that this singularity structure is different from the one in the case of the light pseudoscalar mesons L considered in Ref. [12]. In that case the most important low-energy singularity is the cut due to the πL intermediate state (also shown in Fig. 1 starting at $\nu = M_\pi$ for all particles): the closest single pole is due to the exchange of a vector meson, but is at higher ν values.

For the case of the nucleon we can rely on existing calculations of the infinite volume πN scattering amplitude to one loop and on the knowledge of the low-energy constants (LEC) appearing therein. In particular we show how the application of the so-called subthreshold expansion — very well known in the phenomenology — leads to a particularly simple formula for FVC of the nucleon mass. The solid phenomenological knowledge of the subthreshold coefficients allows a very precise determination of the FVC at or near the physical value of the quark mass. In our numerical analysis we show how the error in the evaluation of the FVC increases as we go to higher quark masses and identify the LEC which control these effects. In particular a better understanding of the quark mass dependence of the axial-vector coupling constant of the nucleon would lead to a much better control of the FVC. The relevance of this issue for the calculation of the FVC for the nucleon mass has been already discussed at length in Ref. [16], where we presented preliminary results (dating already five years back). Indeed until lattice calculations of g_A at lower quark masses were published, we were not able to present a reliable numerical analysis of these FVC. The situation has now clearly improved, but is not yet fully satisfactory and we do think that there is still a lot to be understood about the behavior of g_A and other nucleon-related quantities as functions of the quark mass.

Only very few publications on finite volume effects for heavy mesons exist so far [18–22], most of which are not concerned with the FVC to the mass. Also about the scattering amplitude of pions off heavy mesons a lot less is known, even only in the low-energy region. We give the expression of the tree level scattering amplitude and show how the Lüscher formula needs to be modified if one considers the heavy mesons away from the infinite mass limit (*i.e.* as nondegenerate). We show that also in this case one can define a subthreshold expansion completely analogous to the case of the nucleon, and express the FVC in terms of the subthreshold parameters, so emphasizing the close analogy between the two cases. We provide a simple numerical analysis on the basis of the limited information which is available on the $\pi H H^*$ (for $H = D$ or B mesons) coupling constant and discuss the difference between the fully relativistic case and the nonrelativistic limit of the Lüscher formula.

2 Resummed Lüscher formula for the nucleon mass

In this section we present and discuss the formula we will use for analyzing the finite volume effects on the nucleon mass numerically. We rely on the resummed version of the Lüscher formula [8, 9] which has been proposed in Ref. [12]. The formula for the relative finite volume correction $R_N \equiv (m_N(L) - m_N)/m_N$ reads as follows:

$$R_N = \frac{3\varepsilon_\pi^2}{4\pi^2} \sum_{n=1}^{\infty} \frac{m(n)}{\sqrt{n}\lambda_\pi} \left[2\pi\varepsilon_\pi g_{\pi N}^2 e^{-\sqrt{n(1-\varepsilon_\pi^2)}\lambda_\pi} - \int_{-\infty}^{\infty} dy\, e^{-\sqrt{n(1+y^2)}\lambda_\pi} \tilde{D}^+(y) \right] \quad (2)$$

where

$$\varepsilon_\pi = \frac{M_\pi}{2m_N} \ , \quad \lambda_\pi = M_\pi L \ , \quad \tilde{D}^+(y) = m_N D^+(iM_\pi y, 0) \quad (3)$$

where D^+ is one of the components of the elastic πN scattering amplitude, which is defined as

$$T(\pi^a(q)N(p) \to \pi^{a'}(q')N(p')) \equiv T_{a'a} = \delta_{a'a}T^+ + \frac{1}{2}[\tau_{a'}, \tau_a]T^- \ . \quad (4)$$

Each of the two isospin components is then broken down into

$$T^\pm = \bar{u}' \left[D^\pm(\nu, t) - \frac{1}{4m_N}[\slashed{q}', \slashed{q}]B^\pm(\nu, t) \right] u \quad (5)$$

and each of the amplitudes depends on the kinematical variables t and ν, defined as:

$$t = (q - q')^2 \ , \quad \nu = \frac{s - u}{4m_N} \ , \quad \text{where} \quad s = (p + q)^2 \ , \quad u = (p - q')^2 \ . \quad (6)$$

The term with $n = 1$ in Eq. (2) has been first given by Lüscher [8] as an application of his general formula for finite size corrections to masses [9], but with a factor 2 missing in the first term within the brackets. This has been pointed out in Ref. [14] and later confirmed in Ref. [15] — it is indeed easy to follow the steps in Lüscher's general proof [9] adapting it to the present case and derive formula (2) as it stands.

n	1	2	3	4	5	6	7	8	9	10	11	12	13	14	15
$m(n)$	6	12	8	6	24	24	0	12	30	24	24	8	24	48	0

Table 1: The multiplicities $m(n)$ for $n \le 15$.

The extension to the exponentially suppressed terms with $n > 1$ can be immediately obtained following the general derivation given in Ref. [12]. They appear weighted by the multiplicities $m(n)$ — these are easily calculable and are reproduced here for convenience in Table 1 for $n \leq 15$.

The resummed version of the formula exactly reproduces the one-loop result in ChPT if the tree level scattering amplitude is inserted in the integral in (2), see Ref. [12]. In the present case, due to the special counting rules in the one-nucleon sector, the πN amplitude receives tree level contributions both at order p as well as at order p^2. Inserting the πN amplitude up to order p^2 one can indeed exactly reproduce the calculation of the $O(p^3)$ and $O(p^4)$ finite volume corrections performed in Ref. [14]. Since the πN amplitude is known well beyond the $O(p^2)$ level, in fact up to $O(p^4)$ [23], one can use this formula to go beyond the one-loop level. In this manner the corrections beyond $O(p^4)$ will be given exactly as far as the first three leading exponential terms are concerned, and only approximately for the subleading exponential terms beyond $e^{-\sqrt{3}M_\pi L}$ [12]. Based on the analysis in Ref. [17] we expect the contributions which go beyond the resummed formula (2) to be numerically small.

As seen in (2,3), the πN amplitude is needed here in a particular kinematical configuration, namely for $t = 0$ and for ν purely imaginary and small: the contributions with large values of ν are suppressed by the exponential kernel in the integral in (2). It is therefore natural to make a Taylor expansion of the amplitude around $\nu = 0$ after having subtracted the pole due to the one-nucleon exchange diagram (also called the Born term). Such an expansion is in fact already well known in the phenomenology and is referred to as the subthreshold expansion. It reads as follows

$$D^+(\nu, 0) = D^+_{\mathrm{pv}}(\nu, 0) + D^+_{\mathrm{p}}(\nu, 0) + D^+_{\mathrm{na}}(s, u) \tag{7}$$

where

$$
\begin{aligned}
D^+_{\mathrm{pv}}(\nu, 0) &= \frac{g^2_{\pi N}}{m_N} \frac{\nu^2_B}{\nu^2_B - \nu^2} \\
D^+_{\mathrm{p}}(\nu, 0) &= d^+_{00} + d^+_{10}\nu^2 + d^+_{20}\nu^4
\end{aligned} \tag{8}
$$

and $\nu_B = -M^2_\pi/(2m_N)$. The function $D^+_{\mathrm{na}}(s, u)$ contains the analytically nontrivial part of the amplitude. Up to order p^4 in the chiral expansion this can be written as a sum of two single variable functions:

$$D^+_{\mathrm{na}}(s, u) = D^+_1(s) + D^+_1(u) + O(p^5) \tag{9}$$

which admit the following dispersive representation:

$$D^+_1(s) = \frac{\nu^5}{\pi} \int_{M_\pi}^{\infty} d\nu' \frac{\mathrm{Im}D^+_1(s')}{\nu'^5(\nu' - \nu - i\epsilon)} \tag{10}$$

where $s' = 2m_N\nu' + m_N^2 + M_\pi^2$. This representation shows that, due to the large number of subtractions, the function D_1^+ is small near $\nu = 0$. As we will see later, its contribution to the finite size shift of the nucleon mass is negligible.

This observation leads to the following expression for the relative finite volume shift R_N:

$$R_N = \frac{3\varepsilon_\pi^2}{4\pi^2} \sum_{n=1}^{\infty} \frac{m(n)}{\sqrt{n}\lambda_\pi} \left[g_{\pi N}^2 \varepsilon_\pi \left(2\pi e^{-\sqrt{n(1-\varepsilon_\pi^2)}\lambda_\pi} - \varepsilon_\pi I_{\mathrm{pv}}(\sqrt{n}\lambda_\pi, \varepsilon_\pi) \right) \right. \tag{11}$$

$$\left. - \bar{d}_{00}^+ B^0(\sqrt{n}\lambda_\pi) + \bar{d}_{10}^+ B^2(\sqrt{n}\lambda_\pi) - \bar{d}_{20}^+ B^4(\sqrt{n}\lambda_\pi) \right] + R_{N,\mathrm{na}}$$

where

$$I_{\mathrm{pv}}(\lambda_\pi, \varepsilon_\pi) = \int_{-\infty}^{\infty} dy \frac{e^{-\sqrt{(1+y^2)}\lambda_\pi}}{\varepsilon_\pi^2 + y^2} \ , \quad B^k(\lambda_\pi) = \int_{-\infty}^{\infty} dy \, y^k e^{-\sqrt{(1+y^2)}\lambda_\pi} \tag{12}$$

are the relevant finite volume integrals, $\bar{d}_{i0}^+ = m_N M_\pi^{2i} d_{i0}^+$ and $R_{N,\mathrm{na}}$ is the remainder coming from the (subtracted) analytically nontrivial part of the amplitude.

If we neglect the contribution $R_{N,\mathrm{na}}$ the representation (11) is very simple and expresses the finite volume shift of the nucleon mass in terms of only a handful of physical observables: the pion and proton masses, M_π, m_N, the pion–nucleon coupling constant $g_{\pi N}$ and the three subthreshold parameters $\bar{d}_{i0}^+$. If one knows the low-energy constants which appear in the chiral representation of these quantities, one can predict their quark mass dependence and therefore the finite volume shift R_N as a function of the quark mass. We also stress that for simulations performed at the physical point, Eq. (11) allows an evaluation of the FVC based only on input extracted from the phenomenology, and indeed on rather well known quantities like $g_{\pi N}$ and the subthreshold coefficients.

3 Quark mass dependence of m_N, g_A, $g_{\pi N}$ and the subthreshold coefficients

The chiral representation for the observables m_N, $g_{\pi N}$ up to order p^4 can be found in Ref. [23, 24] and will be reproduced here for convenience. It reads

as follows:

$$
\begin{aligned}
m_N &= m - 4c_1 M^2 - \frac{3g^2 M^3}{32\pi F^2} + \left[\tilde{e}_1 - \frac{3(2g^2 - c_2 m)}{8NF^2} \right] M^4 + \mathcal{O}(M^5) \\
g_{\pi N} &= \frac{g_A m_N}{F_\pi} \left(1 - \frac{2d_{18} M^2}{g} + \mathcal{O}(M^4) \right)
\end{aligned}
\tag{13}
$$

where $N = 16\pi^2$, the symbols m, g and F indicate the nucleon mass, the axial coupling constant and the pion decay constant in the SU(2) chiral limit, whereas $M^2 = 2B\hat{m}$ is the leading term in the expansion of the pion mass square in powers of the quark mass. The LEC c_i, d_i and e_i appear in the chiral Lagrangian in the one-nucleon sector at order p^2, p^3 and p^4 respectively, and the tildas indicate renormalized, scale independent versions thereof [23] (the c_i's as well as d_{18} are scale independent — see appendix A for more details).

For the axial charge, the order p^5 result[1] is partially known [25] and will be used in the following,

$$
g_A = g \left[1 + (\alpha_2 L_\chi + \beta_2) M_\pi^2 + \alpha_3 M_\pi^3 + \left(\alpha_4 L_\chi^2 + \gamma_4 L_\chi + \beta_4 \right) M_\pi^4 \right]
\tag{14}
$$

with $L_\chi = \frac{1}{NF^2} \ln \left(\frac{M_\pi}{\mu} \right)$ and

$$
\alpha_2 = -2(1 + 2g^2) , \quad \alpha_3 = \frac{3(1 + g^2) - 4m(c_3 + 2c_4)}{24\pi F^2 m} , \quad \alpha_4 = \frac{8}{3} + \frac{37}{3}g^2 + 16g^4
$$

$$
\beta_2 = \frac{4}{g} d_{16}^r(\mu) - \frac{g^2}{NF^2} , \qquad \beta_4 = \frac{c_4}{m} \frac{4}{NF^2} + \frac{2g^2}{(NF^2)^2} \bar{\ell}_4 + f ,
$$

$$
\gamma_4 = \frac{4(c_4 - c_3)}{m} - 12 d_{16}^r(\mu) \left(\frac{5}{3g} + g \right) - \frac{2}{F^2} \alpha_2 \bar{\ell}_4 .
\tag{15}
$$

Note that the above expressions for γ_4 and β_4 do not represent the full $\mathcal{O}(p^5)$ result. We introduce a generic LEC f which collects all the polynomial contributions proportional to M_π^4. The chiral expansion of the subthreshold coefficients reads:

$$
\begin{aligned}
d_{00}^+ &= -\frac{2(2c_1 - c_3)M_\pi^2}{F_\pi^2} + \frac{g^2 (3 + 8g^2) M_\pi^3}{64\pi F_\pi^4} + \\
&\quad + M_\pi^4 \left[\frac{\tilde{e}_3}{F_\pi^2} - \frac{c_1}{8\pi^2 F_\pi^4} \bar{\ell}_3 + \frac{3 (g^2 + 6g^4)}{64\pi^2 F_\pi^4 m} - \frac{2c_1 - c_3}{16\pi^2 F_\pi^4} \right]
\end{aligned}
$$

---

[1]We refer here to the counting in the Lagrangian. As seen in Eq. (14) this translates into an expression including up to the $O(M_\pi^4)$ correction in g_A.

$$d_{10}^+ = \frac{2c_2}{F_\pi^2} - \frac{(4+5g^4)\,M_\pi}{32\pi F_\pi^4} +$$

$$+ M_\pi^2 \left[\frac{\tilde{e}_4}{F_\pi^2} - \frac{16c_1c_2}{F_\pi^2 m} - \frac{1+g^2}{4\pi^2 F_\pi^4 m} - \frac{197g^4}{240\pi^2 F_\pi^4 m} \right]$$

$$d_{20}^+ = \frac{12+5g^4}{192F_\pi^4 M_\pi\pi} + \frac{\tilde{e}_6}{F_\pi^2} + \frac{17+10g^2}{24\pi^2 F_\pi^4 m} + \frac{173g^4}{280\pi^2 F_\pi^4 m} \qquad (16)$$

3.1 Determination of the LEC

The LEC from the nucleon sector are determined by fitting the chiral representations of m_N, g_A, $g_{\pi N}$ and d_{i0}^+ to experimental data and results from lattice simulations (on m_N and g_A only). Details of the fits are given in appendix B.

In order to have a better handle on the uncertainties, we perform a fit to the order p^2 chiral representations as well as to the complete formulae indicated in Eqs. (13),(14) and (16). Note that in the following, we give the value for the scale independent $\bar{d}_{16}$ evaluated at the physical pion mass (see appendix A) while for the higher order LEC we indicate the values of $e_i^r(\mu), f(\mu)$ at $\mu = M_\rho$.

- At order p^2, we obtain

$$m = 0.896 \pm 0.003\,\mathrm{GeV} \qquad\qquad g = 1.126 \pm 0.007$$
$$c_1 = -0.54 \pm 0.04\,\mathrm{GeV}^{-1} \qquad c_2 = 1.79 \pm 0.03\,\mathrm{GeV}^{-1}$$
$$c_3 = -3.37 \pm 0.18\,\mathrm{GeV}^{-1} \qquad \bar{d}_{16} = 0.06 \pm 0.11\,\mathrm{GeV}^{-2}$$
$$d_{18} = -1.13 \pm 0.19\,\mathrm{GeV}^{-2}$$
$$\chi^2/\mathrm{d.o.f.} = 5.7/7 \qquad\qquad\qquad\qquad\qquad (17)$$

  Note that the term proportional to M_π^2 in g_A is also included in the order p^2 fit, although it is a term of order p^3. Furthermore, for the subthreshold coefficients, only the leading terms of the chiral expansion are retained at order p^2. In particular, $d_{20}^+ = 0$.

- The fit with the untruncated expressions of Sec. 3 does not allow one to determine all of the appearing LEC. We have checked that if one holds three of the LEC at a constant value then the fit becomes stable. We choose to fix the three LEC c_2, c_3 and c_4. To assess the uncertainties thereby introduced into the analysis, we use two different sets of values

9

for these three LEC, given in Ref. [23],

$$\text{Set I} \quad c_2 = 1.7 \, \text{GeV}^{-1} \ , \quad c_3 = -3.6 \, \text{GeV}^{-1} \ , \quad c_4 = 2.1 \, \text{GeV}^{-1} \ ,$$
$$\text{Set II} \quad c_2 = 2.7 \, \text{GeV}^{-1} \ , \quad c_3 = -4.5 \, \text{GeV}^{-1} \ , \quad c_4 = 2.4 \, \text{GeV}^{-1} \ .$$

In the following, this fit will be referred to as the order p^4 fit, although the formulae also contain terms of higher order. For set I, the fit yields

$$
\begin{aligned}
m &= 0.907 \pm 0.021 \, \text{GeV} & g &= 1.201 \pm 0.077 \\
c_1 &= -0.56 \pm 0.30 \, \text{GeV}^{-1} & \bar{d}_{16} &= -3.05 \pm 1.54 \, \text{GeV}^{-2} \\
d_{18} &= -1.20 \pm 0.22 \, \text{GeV}^{-2} & f &= 3.2 \pm 47 \, \text{GeV}^{-4} \\
e_1^r &= 15 \pm 13 \, \text{GeV}^{-3} & e_3^r &= -34 \pm 72 \, \text{GeV}^{-3} \\
e_4^r &= 37 \pm 16 \, \text{GeV}^{-3} & e_6^r &= 23.2 \pm 1.4 \, \text{GeV}^{-3} \\
\chi^2/\text{d.o.f.} &= 4.8/5 &&
\end{aligned}
\tag{18}
$$

while for set II we find

$$
\begin{aligned}
m &= 0.905 \pm 0.021 \, \text{GeV} & g &= 1.207 \pm 0.077 \\
c_1 &= -0.60 \pm 0.30 \, \text{GeV}^{-1} & \bar{d}_{16} &= -3.43 \pm 1.56 \, \text{GeV}^{-2} \\
d_{18} &= -1.2 \pm 0.2 \, \text{GeV}^{-2} & f &= -0.1 \pm 47 \, \text{GeV}^{-3} \\
e_1^r &= 15 \pm 13 \, \text{GeV}^{-3} & e_3^r &= 56 \pm 72 \, \text{GeV}^{-3} \\
e_4^r &= -86 \pm 20 \, \text{GeV}^{-3} & e_6^r &= 23.2 \pm 1.4 \, \text{GeV}^{-3} \\
\chi^2/\text{d.o.f.} &= 4.8/5 &&
\end{aligned}
\tag{19}
$$

The errors indicated for the LEC are statistical only and do not account, in particular, for the uncertainties due to higher order effects. The statistical error quoted above most likely underestimates the real uncertainties. Comparing the different resulting values of LEC, one observes that the nucleon mass in the chiral limit lies very close to $0.9 \, \text{GeV}$ in all three fits. Also the values for c_1 end up quite close together, but fall out of the error bars for c_1 quoted in Ref. [26]. However, given the fact that the c_i are correlated, we should compare with the value of c_1 given in Ref. [23], which is in better agreement. Our fits with the two sets of order p^2 LEC lead to consistent results for c_1. The LEC of the order p^3 chiral Lagrangian are less well known. Comparing with Ref. [27], the values of $\bar{d}_{16}$ of the order p^4 fits agree remarkably well. In the order p^2 fit, the resulting value of $\bar{d}_{16}$ is not reconcilable with phenomenology (see also Ref. [16]). We come to the same conclusion as the authors of Ref. [25]. Only the inclusion of the partial order p^5 corrections in g_A leads to a reasonable fit. The coupling d_{18} is in agreement with the

range of values found in Ref. [28]. Since d_{18} is determined with the help of the Goldberger–Treiman relation at the physical point, different values of d_{18} merely reflect different values of g. As for the LEC of the order p^4 chiral Lagrangian in the nucleon sector, the huge statistical errors of the fits confirm that they are basically unknown.

3.2 Numerical analysis

Given the values of the LEC from the fits, we plot the quark mass dependence of the quantities m_N, g_A and the subthreshold coefficients. As can be seen in Fig. 2, the nucleon mass is described remarkably well by the order p^2 curve which is just a quadratic function in the pion mass. Fig. 2 also shows the axial charge. It exhibits the mild quark mass dependence observed in lattice calculations already at order p^2 and stays within the order p^4 error bars over a wide range of quark masses. However, this picture hides the fact that the chiral series of g_A is not well behaved, as the observed smooth behavior is the result of compensations among different chiral orders. We believe, however, that it is rather unlikely to have a strong quark mass dependence in the region between the physical pion mass and the present lowest lattice values (around $M_\pi \sim 0.3$ GeV). As we will show in the next section the present knowledge on the quark mass dependence of g_A (which is based mainly on lattice calculations, rather than on chiral predictions) does allow us to calculate the FVC for the nucleon mass sufficiently reliably. In the latter it is actually the pion nucleon coupling constant which appears and Fig. 3 shows that its quark mass dependence is rather weak and that the difference between the two sets is negligible.

The behavior of the subthreshold coefficients d_{00}^+ and d_{10}^+ beyond the physical point is not predicted by chiral symmetry. Going from set I to set II leads to substantial changes in the higher order LEC and therefore to a very different behavior as a function of the quark mass. However, the extrapolation towards the chiral limit seems to work quite well. The coefficient d_{20}^+ seems to be in much better shape as it does not depend on the c_i. Set I and set II almost yield identical results. However, this nice agreement should not mislead one into thinking that everything is under control here: large higher order corrections may modify this nice picture, since Eq. (16) is the leading order result for d_{20}^+. For instance, replacing F_π by its value in the chiral limit in d_{20}^+ yields the dashed-dotted curve in Fig. 4. Note that the coupling e_6 was readjusted to reproduce the correct physical value.
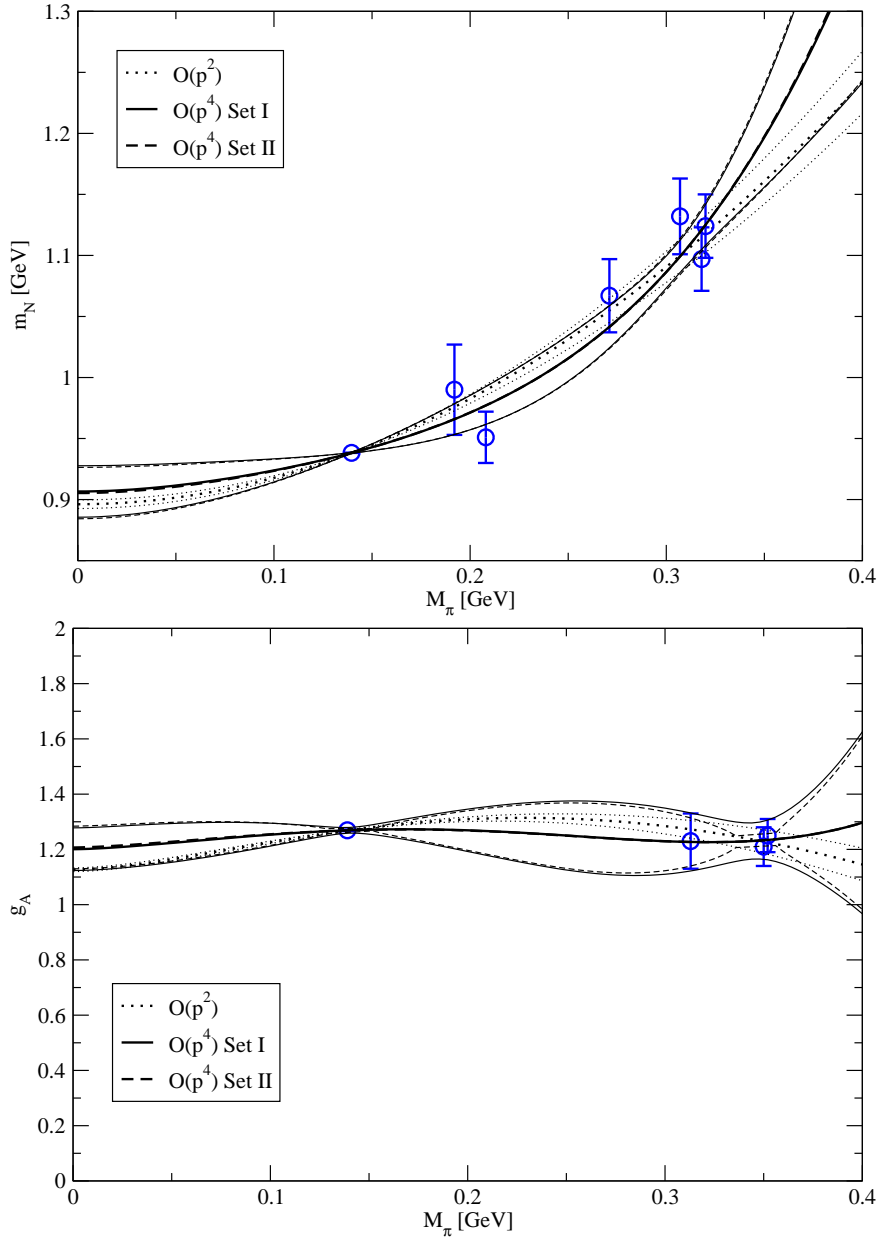
Figure 2: The upper panel shows the quark mass dependence of the nucleon mass and the lower panel of the axial charge, respectively. The dotted lines show the results of the order p^2 fit, the solid lines represent order p^4 set I and the dashed lines are order p^4 set II. The error bands are represented by thinner lines plotted with the same line style as the central value. The circles show the lattice result as well as the physical point used as input.
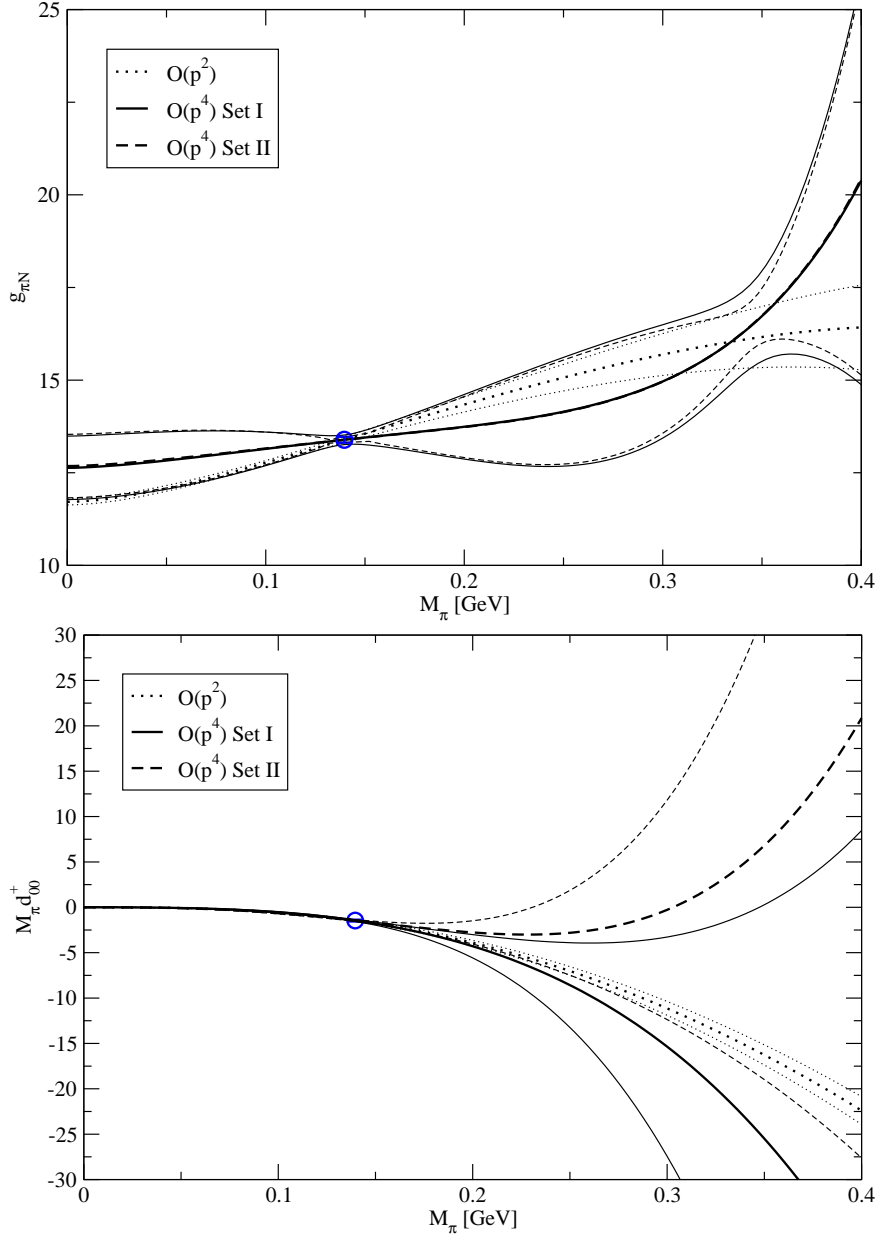
Figure 3: The upper panel shows the quark mass dependence of the pion nucleon coupling constant and the lower panel of the scaled subthreshold coefficient $M_\pi d_{00}^+$, respectively. The dotted lines show the results of the order p^2 fit, the solid lines represent order p^4 set I and the dashed lines are order p^4 set II. The error bands are represented by thinner lines plotted with the same line style as the central value. The circles show the physical value used as input.
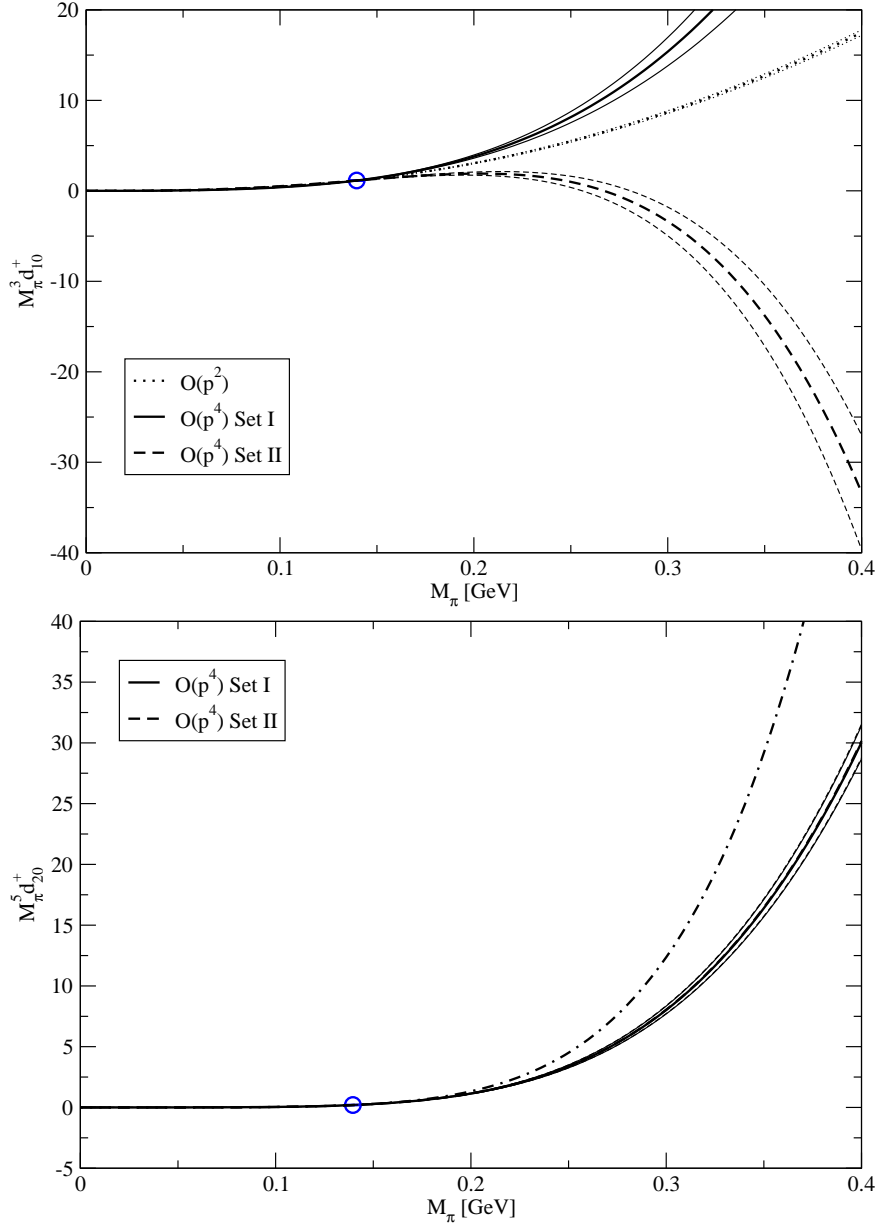
Figure 4: The upper panel shows the quark mass dependence of the scaled subthreshold coefficient $M_\pi^3 d_{10}^+$ and the lower panel of $M_\pi^5 d_{20}^+$, respectively. The dotted lines show the results of the order p^2 fit, the solid lines represent order p^4 set I and the dashed lines are order p^4 set II. The error bands are represented by thinner lines plotted with the same line style as the central value. The circles show the physical value used as input. The dashed-dotted line shows the rescaled coefficient d_{20}^+ with F_π replaced by F, as described in the main text.

14

4 Numerical analysis of the FVC to the nucleon mass

With the quark mass dependence of all the quantities appearing in Eq. (11) established, the finite volume effects can now be calculated for pion masses below ~ 0.4 GeV and box sizes $L > 2$ fm. In Fig. 5 we show the finite volume effects for boxes of spatial extent $L = 2, 3$ fm. To illustrate the size of the different contributions to the FVC, we break down the corrections into the different terms of Eq. (11). This is shown in Fig. 6. The contributions from the Born term dominate the finite volume effects and are practically the same for all three fits. Since the quark mass dependence of the subthreshold coefficients is almost unknown, their contributions to the finite volume effects vary a lot. The shift from the order p^2 fit to the order p^4 fits is mainly due to a vanishing contribution from d_{20}^+ at order p^2. Removing this shift by setting d_{20}^+ to its physical value brings the order p^2 curve down into the error bars of the order p^4 fits.

At order p^4, the fit with set I shows cancellations between d_{10}^+ and d_{20}^+. However, these cancellations are absent for set II, where d_{00}^+ and d_{10}^+ contribute very little but the contribution from d_{20}^+ stays the same as in set I. This leads to the large difference between set I and set II. The central values shift by twice the error bars. It is obvious that a precise prediction of the finite size effects is very difficult away from the physical point. One also observes that the finite size effects strongly depend on the values of the LEC c_i, $i = 2, 3, 4$ through the subthreshold coefficients. Therefore, if the finite volume effects are well determined by lattice simulations, this would provide useful constraints and possibly a determination of (some combinations of) the c_i.

If we expand our formula for R_N and keep in the scattering amplitude only the $O(p^2)$ contributions we agree exactly with the one in Ref. [14]. A comparison of the numerics at this order is therefore uninteresting (since by inserting the same values for the LEC one trivially gets the same). We stress, however, that as our plots in Fig. 5 indicate, by truncating the chiral expansion at NLO one may get the misleading impression of having rather moderate uncertainties which do not grow very fast with the pion mass. The application of the resummed Lüscher formula allows one to go to higher orders and to verify explicitly that:

- corrections beyond NLO are important;

- the uncertainties grow rather quickly with the pion mass, so that going beyond pion masses of about $0.3 - 0.35$ GeV they become of order 100%.

$M_\pi[\,\mathrm{GeV}]$	$L = 2\,\mathrm{fm}$	$L = 2.5\,\mathrm{fm}$	$L = 3\,\mathrm{fm}$
0.140	$0.090^{+0.002}_{-0.006}{}^{\star}$	$0.041^{+0.001}_{-0.001}{}^{\star}$	$0.0200^{+0.0004}_{-0.0005}$
0.160	$0.082^{+0.006}_{-0.009}{}^{\star}$	$0.036^{+0.002}_{-0.003}$	$0.017^{+0.001}_{-0.001}$
0.180	$0.074^{+0.011}_{-0.013}{}^{\star}$	$0.031^{+0.004}_{-0.004}$	$0.014^{+0.002}_{-0.002}$
0.200	$0.065^{+0.015}_{-0.016}$	$0.027^{+0.005}_{-0.005}$	$0.012^{+0.002}_{-0.002}$
0.220	$0.057^{+0.019}_{-0.019}$	$0.023^{+0.006}_{-0.006}$	$0.010^{+0.002}_{-0.002}$
0.240	$0.050^{+0.022}_{-0.022}$	$0.019^{+0.007}_{-0.007}$	$0.008^{+0.002}_{-0.002}$
0.260	$0.043^{+0.024}_{-0.024}$	$0.016^{+0.007}_{-0.007}$	$0.006^{+0.002}_{-0.002}$
0.280	$0.037^{+0.025}_{-0.026}$	$0.013^{+0.007}_{-0.007}$	$0.005^{+0.002}_{-0.002}$
0.300	$0.031^{+0.026}_{-0.026}$	$0.011^{+0.007}_{-0.007}$	$0.004^{+0.002}_{-0.002}$
0.320	$0.026^{+0.027}_{-0.027}$	$0.009^{+0.007}_{-0.007}$	$0.003^{+0.002}_{-0.002}$
0.340	$0.022^{+0.027}_{-0.027}$	$0.007^{+0.007}_{-0.007}$	$0.002^{+0.002}_{-0.002}$
0.360	$0.019^{+0.028}_{-0.027}$	$0.006^{+0.007}_{-0.007}$	$0.002^{+0.002}_{-0.002}$

Table 2: Our final results for R_N. In the first column, the value of the pion mass is given and in the subsequent columns, the values of R_N for three different sizes of the box are listed. The star indicates that for these values, $M_\pi L < 2$.

We refrain from comparing our error analysis with Ref. [29], where FVC including error bars were calculated at one loop in ChPT. In Ref. [29], plots of the FVC are only given for values of pion masses and box sizes in a region which we consider to lie outside the region of validity of the effective theory.

Our final results are shown in Tab. 2 where we give R_N for different values of pion masses and box sizes. The quoted central value is the average of the central values of set I and set II and the error bars are chosen such that they cover the error bands of both set I and set II.

4.1 Physical point

As we have discussed in detail in the previous sections, the main difficulties in the numerical evaluation of the FVC for the nucleon mass arise from the limited knowledge of the quark mass dependence of the observables which appear in the resummed Lüscher formula. Since several lattice collaborations are reaching or plan to reach the physical value of the pion mass, it is inter-
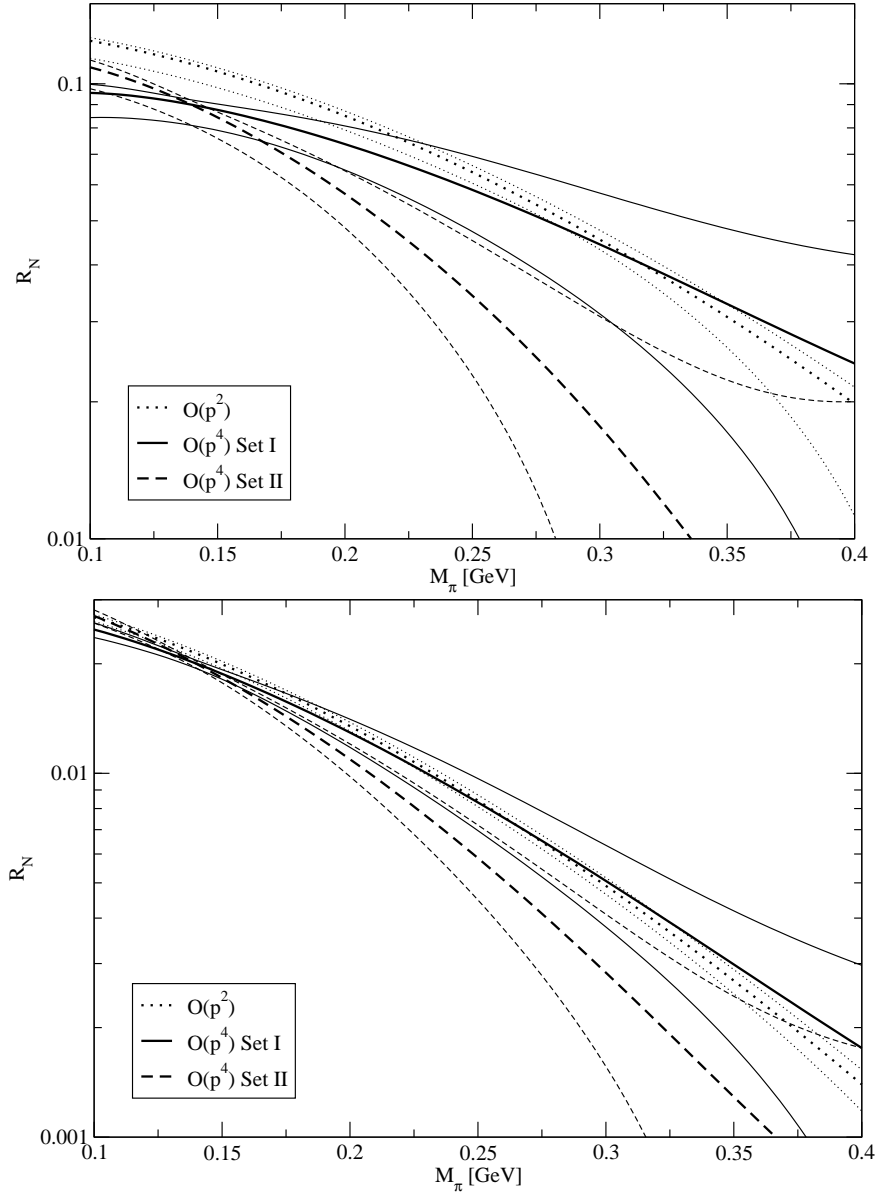
Figure 5: The FVC R_N as a function of the quark mass for $L = 2\,\mathrm{fm}$ (upper panel) and $L = 3\,\mathrm{fm}$ (lower panel). The dotted lines indicate the result of the order p^2 fit, the solid lines are the order p^4 fit with set I and the dashed lines the order p^4 fit with set II, respectively. Note that for $L = 2\,\mathrm{fm}$ and $L = 3\,\mathrm{fm}$, the pion mass should fulfill $M_\pi \geq 0.2\,\mathrm{GeV}$ and $M_\pi \geq 0.13\,\mathrm{GeV}$, respectively, in order to stay in the region of validity of the Lüscher formula.
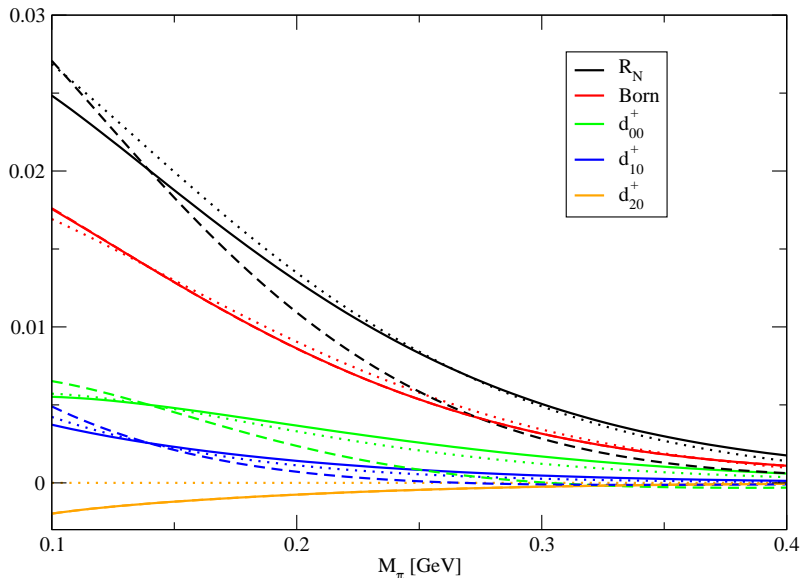
17

Figure 6: Individual contributions to the Lüscher formula (shown by lines of different colors, see legend). The finite volume effect R_N (black lines) is the sum of all the contributions. The line style indicates the order and the set of LEC used. The dotted lines denote the result of the order p^2 fit, the solid lines are the order p^4 fit with set I and the dashed lines the order p^4 fit with set II, respectively. The size of the box is $L = 3\,\mathrm{fm}$ and therefore, the pion mass should fulfill $M_\pi \geq 0.13\,\mathrm{GeV}$ in order to stay in the region of validity of the Lüscher formula.

esting to evaluate the FVC for this case — the advantage of our approach is that at the physical pion mass we can insert directly the measured values for the different observables.

In Fig. 7, R_N is plotted as a function of the size of the box L. The plot shows the order p^2 curves as well as both order p^4 curves. A difference is visible in R_N only because at order p^2, the subthreshold coefficient d_{20}^+ vanishes. The main contribution to the FVC is given by the Born amplitude. The subthreshold coefficients all yield corrections of similar size. In fact, the contributions from d_{10}^+ and d_{20}^+ cancel to a large extent. Since the error bands are constrained very much by the small errors of the experimental input parameters we can predict the FVC very accurately for lattice simulations with physical quark masses in a box of the size $L \geq 3\,\mathrm{fm}$. If nucleon mass calculations with physical quark mass are done in a box of the size $L \geq 3.5\,\mathrm{fm}$ one does not have to worry about finite volume corrections. The effects stay below 1 %.
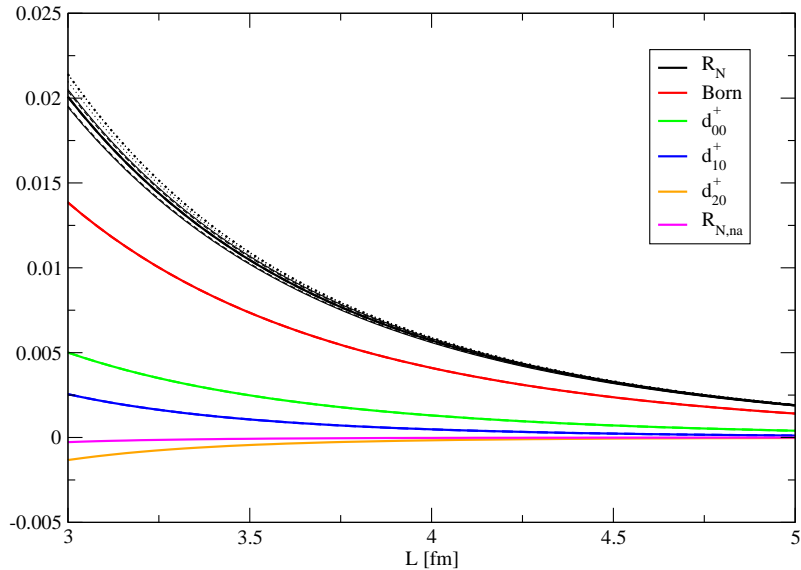
Figure 7: FVC for physical pion mass as a function of the size of the box. The black lines denote R_N. The dotted line is the $O(p^2)$ fit, the solid line and the dashed line are set I and set II of the $O(p^4)$ fit, respectively. The different contributions to the corrections are also plotted, as well as the nonanalytic contributions $R_{N,\mathrm{na}}$ (which are not included in R_N). Note that the difference between the order p^2 and order p^4 curves stems only from d_{20}^+, which vanishes at order p^2.

4.2 Systematic effects

After having evaluated the size of the finite volume effects numerically, we briefly discuss effects which have been neglected in our analysis. There are three different types of systematic corrections:

- We neglect the contributions from the nonanalytic part of the scattering amplitude, $R_{N,\mathrm{na}}$ in Eq. (11).

- Then there are the neglected higher order contributions of the Lüscher formula which vanish as $e^{-\xi M_\pi L}$, with $\xi > \sqrt{3}$.

- Furthermore, the pole of the $\Delta(1232)$ resonance is only taken into account as a polynomial via the LEC in the subthreshold coefficients.

In the following we argue why it is justified to completely neglect the first two of these effects and how we account for the last one.

We show by an explicit calculation that the nonanalytic contributions are very small. It is possible to solve the dispersive integral Eq. (10) in

closed form, as described in Ref. [23]. Removing the fictitious poles from the expression

$$\hat{D}_1^+(s) = \frac{M_\pi}{12 F_\pi^4 m_N \nu^3} \left\{ \Delta_1^+ + g_A^2 \Delta_2^+ + g_A^4 \Delta_3^+ \right\} f(\nu) \qquad (20)$$

with

$$
\begin{aligned}
f(\nu) &= \frac{1}{8\pi} \sqrt{1 - \frac{\nu^2}{M_\pi^2}} \arccos\left(-\frac{\nu}{M_\pi}\right), \\
\Delta_1^+ &= 12\nu^4(-m_N\nu + 3\nu^2 - M_\pi^2), \\
\Delta_2^+ &= 24\nu^4(\nu^2 - M_\pi^2), \\
\Delta_3^+ &= 8(\nu^2 - M_\pi^2)^2(-m_N\nu + 3\nu^2 + M_\pi^2),
\end{aligned}
\qquad (21)
$$

leads to

$$D_1^+(s) = \hat{D}_1^+(s) - \sum_{n=-3}^{4} d_{1,n}^+ \nu^n. \qquad (22)$$

The imaginary part of $D_1^+(s)$ vanishes identically in the Lüscher integral, since it is an odd function in the integration variable. Furthermore, in forward scattering, the contribution from $D_1^+(u)$ is the same as the one from $D_1^+(s)$. Evaluating $R_{N,\mathrm{na}}$ numerically one finds that the contributions of the nonanalytic part of the scattering amplitude to the FVC can safely be neglected in the present analysis.

Higher order terms in the Lüscher formula for finite volume corrections to the pion mass have been explicitly calculated in Ref. [17]. It was found that for $M_\pi L \gtrsim 2$, the contributions which are not included in the resummed Lüscher formula are very small. The formal order of the neglected corrections to the nucleon mass is the same as for the pion mass, $e^{-\xi M_\pi L}$. This suggests that the relative effects of these higher order terms for the nucleon mass are even smaller.

Finally, to estimate the effect of the $\Delta(1232)$ resonance, the particle is included into chiral perturbation theory as an explicit degree of freedom. The resulting tree level scattering amplitude D_Δ^+ can be found in Ref. [24]. Plugging this amplitude into the Lüscher formula Eq. (2) we obtain R_Δ.

In Fig. 8, we compare R_Δ with $R_{\Delta,\mathrm{exp}}$, which is the Lüscher integral over the subthreshold expanded amplitude D_Δ^+. The ratio $P = (R_{\Delta,\mathrm{exp}} - R_\Delta)/R_\Delta$ is shown as a function of the quark mass for different box sizes. The following numerical values (from the set I fit, where relevant) are used for the nucleon and $\Delta(1232)$ masses and the Δ-nucleon coupling:

$$m_N = m \ , \qquad m_\Delta = 1.232\,\mathrm{GeV} \ , \qquad g_{\Delta N} = 13 \ . \qquad (23)$$
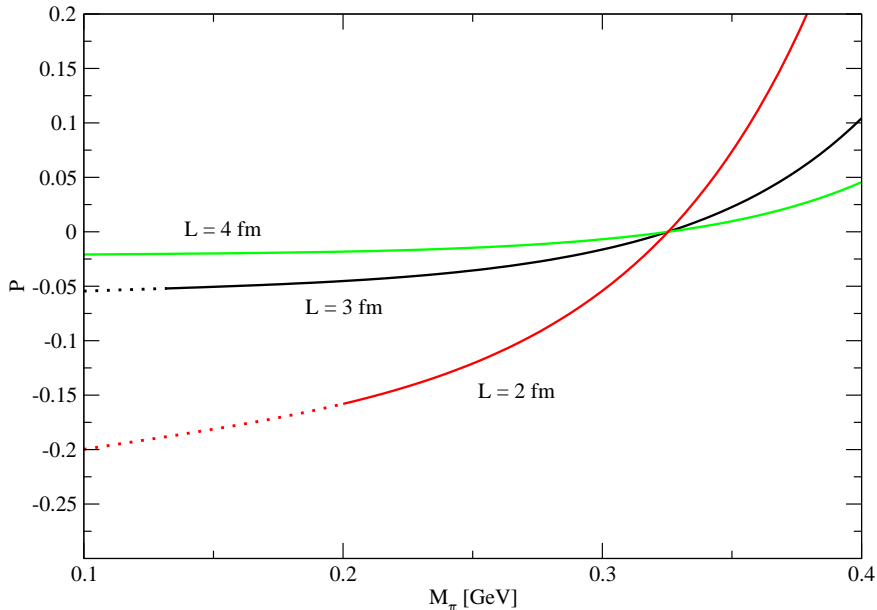
Figure 8: The plot shows the ratio P for different sizes of the box as a function of the pion mass. Note that although P grows fast for larger pion masses, the absolute correction R_Δ vanish exponentially. The LEC from the order p^4 fit set I are used. In the region where the curves are dotted, $M_\pi L < 2$.

Here, a comment is in order. The additional pole of the $\Delta(1232)$ in the scattering amplitude might lead to modifications in the Lüscher formula, as will be described in Sec. 5. For our choice of masses (see Eq. (23)) for the nucleon and the $\Delta(1232)$, this is however not the case.

The corrections are large because for small values of $M_\pi L$, the suppression of the exponential factor in the Lüscher integrand in Eq. (2) is not strong enough. The region with $|\nu|/M_\pi > 1$ — where the subthreshold expansion does not converge anymore — yields sizable contributions. The absolute size of R_Δ compares to a good approximation with the contribution of d_{00}^+, but has the opposite sign. Therefore, the use of the subthreshold expansion in the Lüscher formula leads to a systematic overestimation of the finite size effects if the pole of the $\Delta(1232)$ is not included explicitly in the πN scattering amplitude. We account for this effect by introducing an asymmetric final error $R_N \pm \sigma_{R_N}^\pm$ for the finite size effects,

$$\sigma_{R_N}^+ = \sigma_{R_N} \quad , \qquad \sigma_{R_N}^- = \sqrt{\sigma_{R_N}^2 + (PR_\Delta)^2} \quad . \qquad (24)$$

The definition of σ_{R_N} is provided in appendix B.

21

5 Resummed Lüscher formula for the heavy meson masses

In this section we present a formula that we will use for analyzing the finite volume corrections to the mass of a heavy meson similar to the one in Eq. (2). Again we use a resummed version of the Lüscher formula. In the literature one finds a relativistic [30] as well as a nonrelativistic [31] effective Lagrangian that can be used to calculate the scattering amplitude. They are very briefly introduced in Appendix C, where we also give further references.

Indeed for both formalisms we can provide a Lüscher formula and then calculate the finite volume mass shift. We first discuss the formula that takes the relativistic amplitude as an input. The expression for the relative finite volume correction $R_H^{\rm rel} = (m_H(L) - m_H)/m_H$ in this case reads as follows

$$R_H^{\rm rel} = \frac{M_\pi^2}{32\pi^2 m_H^2} \sum_{n=1}^{\infty} \frac{m(n)}{\sqrt{n}\lambda_\pi} \left[2\pi\bar{\varepsilon}_\pi g_{\pi HH^*}^2 e^{-\sqrt{n(1-\bar{\varepsilon}_\pi^2)}\lambda_\pi} \; \theta(M_\pi^2 + m_H^2 - m_{H^*}^2) \right.$$

$$\left. - \int_{-\infty}^{\infty} dy\, e^{-\sqrt{n(1+y^2)}\lambda_\pi} \tilde{T}^+(y) \right] \;, \quad (25)$$

where

$$\bar{\varepsilon}_\pi = \frac{M_\pi^2 + m_H^2 - m_{H^*}^2}{2m_H M_\pi} \;, \quad \lambda_\pi = M_\pi L \;, \quad \tilde{T}^+(y) = T^+(iM_\pi y, 0). \quad (26)$$

Here and later we adopt the notation that H and H^* stand for any of the heavy pseudoscalar and vector mesons, respectively. The Lüscher formula is valid provided that

$$\Delta_* \equiv m_{H^*} - m_H \geq 0, \qquad M_\pi, \Delta_* \ll m_H, m_{H^*}, \qquad \lambda_\pi \gtrsim 2. \quad (27)$$

The first two relations are well satisfied for all physical masses, while the third one requires $L \gtrsim 3\,\mathrm{fm}$ at the physical pion mass. T^+ is part of the elastic πH scattering amplitude, defined as

$$T(\pi^a(q)H(p) \to \pi^{a'}(q')H(p')) \equiv T_{a'a} = \delta_{a'a}T^+ + \frac{1}{2}[\tau_{a'}, \tau_a]T^- \;, \quad (28)$$

where the amplitudes $T^{\pm}$ depend on ν and t, which are defined similarly as in Eq. (6):

$$t = (q - q')^2 \;, \quad \nu = \frac{s - u}{4m_H} \;, \quad \text{where} \quad s = (p + q)^2 \;, \quad u = (p - q')^2 \;. \quad (29)$$

The proof of this formula is done in the same spirit as in the original article by Lüscher [9]. The crucial difference is that the interaction of a heavy pseudoscalar meson H with a pion is mediated by the heavy vector meson H^*, which has a slightly larger mass than the H. At low energy the pole generated by the H^* exchange is the most important singularity and the one which dominates the Lüscher formula. If one does not take the $m_q \to \infty$ limit and considers H^* as nondegenerate with H, a third mass enters the FVC analysis and leads to some modifications of the proof by Lüscher: the pole that is responsible for the first term in Eq. (25) is shifted outside of the integration contour for some configurations of the meson masses such that its contribution to the mass shift vanishes (see Fig. 1). This is accounted for by the step function. Note that the exponential in the first term can even become complex for some values of the masses, as the constraints given in Eq. (27) do not restrict $\bar{\varepsilon}_\pi$ to values smaller than 1. However, this only occurs for mass values where the step function vanishes such that the resulting mass shift remains real.

We stress that in the degenerate case $m_H = m_{H^*}$ Eq. (25) takes the same form (modulo trivial overall factors) as the one for the nucleon mass — which is the reason for discussing the two in the same paper. What makes this case particularly interesting is precisely the presence of a second almost degenerate mass, whose exact value we are free to vary. By varying it, we can better study and understand the role of the first, exponentially leading term in the Lüscher formula, and ask in particular what happens if we change the masses such that the step function vanishes, and the first term in Eq. (25) disappears. This question is also relevant for the nucleon case if we consider the contribution of the Δ, which we have briefly discussed in Sect. 4.2. Indeed as we vary the pion mass, the Δ mass may get closer (depending on its quark mass dependence) to the nucleon mass and the corresponding pole may move from the right-hand to the left-hand side of the imaginary axis in the ν-plane. It is then a relevant question, what influence this has on the FVC. The dependence of the FVC on the mass difference Δ_* will be discussed below and is illustrated in Fig. 11.

The Lüscher formula takes as input the amplitude in forward direction, i.e. for $t = 0$, and for ν purely imaginary and small, as the contributions for large ν are suppressed due to the exponential in the integrand. Similarly as for the πN amplitude, it is convenient to use the subthreshold expansion of the πH amplitude:

$$T^+(\nu, 0) = T^+_{\mathrm{pv}}(\nu, 0) + T^+_{\mathrm{p}}(\nu, 0) + T^+_{\mathrm{na}}(s, u) , \qquad (30)$$

23

where

$$T_{\mathrm{pv}}^{+}(\nu, 0) = \frac{g_{\pi HH^*}^2 \nu_C^2}{\nu_C^2 - \nu^2} \ ,$$

$$T_{\mathrm{p}}^{+}(\nu, 0) = t_{00}^+ + t_{10}^+ \nu^2 + t_{20}^+ \nu^4 \ , \tag{31}$$

with

$$\nu_C = -\bar{\varepsilon}_\pi M_\pi = -\frac{M_\pi^2 + m_H^2 - m_{H^*}^2}{2m_H} \ . \tag{32}$$

In contrast to the subthreshold expansion for the πN amplitude, there is no inverse mass factor in the definition of T_{pv}^+, because here the amplitude is dimensionless. In order to have a dimensionless coupling constant $g_{\pi HH^*}$, we also need to apply a definition that is somewhat different from the usual one, namely

$$g_{\pi HH^*}^2 = \lim_{\nu^2 \to \nu_C^2} \frac{\nu_C^2 - \nu^2}{\nu_C^2} \, T \ . \tag{33}$$

Inserting the subthreshold expansion in the formula for the mass shift in Eq. (25), we get

$$R_H^{\mathrm{rel}} = \frac{M_\pi^2}{32\pi^2 m_H^2} \sum_{n=1}^{\infty} \frac{m(n)}{\sqrt{n}\lambda_\pi}$$

$$\times \left[g_{\pi HH^*}^2 \bar{\varepsilon}_\pi \left(2\pi e^{-\sqrt{n(1-\bar{\varepsilon}_\pi^2)}\lambda_\pi} \, \theta(M_\pi^2 + m_H^2 - m_{H^*}^2) - \bar{\varepsilon}_\pi I_{\mathrm{pv}}(\sqrt{n}\lambda_\pi, \bar{\varepsilon}_\pi) \right) \right.$$

$$\left. - \bar{t}_{00}^+ B^0(\sqrt{n}\lambda_\pi) + \bar{t}_{10}^+ B^2(\sqrt{n}\lambda_\pi) - \bar{t}_{20}^+ B^4(\sqrt{n}\lambda_\pi) \right] + R_{H,\mathrm{na}} \ . \tag{34}$$

The finite volume integrals I_{pv} and B^k are the same as in Eq. (12). Furthermore, $\bar{t}_{i0}^+ = M_\pi^{2i} t_{i0}^+$ and $R_{H,\mathrm{na}}$ is the remainder coming from the analytically nontrivial part of the amplitude.

At tree level, we find for the subthreshold coefficients

$$t_{00}^+ = \frac{g_{\pi HH^*}^2 (m_H \nu_C + 2M_\pi^2)\nu_C}{m_H(M_\pi^2 - \nu_C^2)}, \qquad t_{10}^+ = t_{20}^+ = 0 \ , \tag{35}$$

with the coupling constant given by

$$g_{\pi HH^*}^2 = \frac{3g^2 m_H^3}{F_\pi^2 m_{H^*}^2 \nu_C}(\nu_C^2 - M_\pi^2) \ . \tag{36}$$

Furthermore, $T_{\mathrm{na}}^+(s, u) = 0$, as no nonanalytical contributions can come from tree level graphs, which then implies that $R_{H,\mathrm{na}} = 0$.

The expression for the relative finite volume correction $R_H^{\mathrm{nrel}} = (m_H(L) - m_H)/m_H$ in the nonrelativistic formalism reads

$$R_H^{\mathrm{nrel}} = -\frac{M_\pi^2}{32\pi^2 m_H} \sum_{n=1}^{\infty} \frac{m(n)}{\sqrt{n}\lambda_\pi} \int_{-\infty}^{\infty} dy\, e^{-\sqrt{n(1+y^2)}\lambda_\pi} \tilde{T}^+(y) \,. \qquad (37)$$

Note that the absolute mass difference $m_H R_H^{\mathrm{nrel}}$ is now independent of m_H. The term proportional to $g_{\pi HH^*}^2$ has disappeared because the argument of the step function is always negative if we take the limit $m_H \to \infty$ at fixed Δ_* (no matter how small it is).

The proof of the Lüscher formula only depends on the positions of the poles of the propagators, which are the same also in the nonrelativistic theory. Thus there is no need to repeat the full proof, all we have to do is to expand the absolute mass difference $m_H R_H^{\mathrm{nrel}}$ in Eq. (25) to leading order in $1/m_H$. As pointed out in Appendix C, the fields used for the two Lagrangians differ in normalization and to compensate for this we have to absorb a factor $1/m_H$ into the scattering amplitude $\tilde{T}^+$.

Because the nonrelativistic amplitude has mass dimension -1, we have again to change the definition of the coupling $g_{\pi HH^*}$ to

$$g_{\pi HH^*}^2 = \lim_{\nu^2 \to \Delta_*^2} \frac{\Delta_*^2 - \nu^2}{\Delta_*} \, T \,, \qquad (38)$$

which is dimensionless. This redefinition then leads to

$$T_{\mathrm{pv}}^+(\nu, 0) = \frac{g_{\pi HH^*}^2 \Delta_*}{\Delta_*^2 - \nu^2}. \qquad (39)$$

Inserting the subthreshold expansion in the formula for the finite volume effect in Eq. (37), we get

$$R_H^{\mathrm{nrel}} = \frac{M_\pi^2}{32\pi^2 m_H} \sum_{n=1}^{\infty} \frac{m(n)}{\sqrt{n}\lambda_\pi} \left[-\frac{g_{\pi HH^*}^2}{\Delta_*} \tilde{\varepsilon}_\pi^2 I_{\mathrm{pv}}(\sqrt{n}\lambda_\pi, \tilde{\varepsilon}_\pi) \right.$$

$$\left. - \bar{t}_{00}^+ B^0(\sqrt{n}\lambda_\pi) + \bar{t}_{10}^+ B^2(\sqrt{n}\lambda_\pi) - \bar{t}_{20}^+ B^4(\sqrt{n}\lambda_\pi) \right] + R_{H,\mathrm{na}} \,. \quad (40)$$

The finite volume integrals I_{pv} and B^k are again the same as in Eq. (12) and

$$\tilde{\varepsilon}_\pi = -\frac{\Delta_*}{M_\pi} \,. \qquad (41)$$

Also, $\bar{t}_{i0}^+ = M_\pi^{2i} t_{i0}^+$ and $R_{H,\mathrm{na}}$ is the remainder coming from the analytically nontrivial part of the amplitude.

From the nonrelativistic Lagrangian we then get at tree level,

$$t_{00}^+ = \frac{g_{\pi HH^*}^2 \Delta_*}{M_\pi^2 - \Delta_*^2}, \qquad\qquad t_{10}^+ = t_{20}^+ = 0 , \qquad (42)$$

$$g_{\pi HH^*}^2 = \frac{3g^2}{F_\pi^2}(\Delta_*^2 - M_\pi^2) , \qquad\qquad T_{\mathrm{na}}^+(s,u) = 0, \qquad (43)$$

These results are identical to the leading term in the $1/m_H$ expansion of the corresponding relativistic expressions (up to factors of m_H and Δ_* due to the normalization of the heavy meson field and the differing definition of $g_{\pi HH^*}$, respectively).

6 Numerical analysis of the FVC to the heavy meson masses

The finite volume effects can now be calculated for arbitrary pion and heavy meson masses and box sizes L within the validity of chiral perturbation theory. To get meaningful results, one has to ensure that the conditions given in Eq. (27) are respected.

For the coupling constant g a number of values from different sources are available in the literature (see Refs. [32–38]). g depends on both the mass of the heavy and the light quark, and neither dependence is fully understood. The listed publications give values for g for different heavy quark and light quark masses and, including also the error bars, these range from 0.18 to 0.79. For the numerical results presented in the following, we have used $g = 0.5$ everywhere and thus neglected any quark mass dependence.

Figs. 9 and 10 show the finite volume effects for the D and B meson as a function of the pion mass for box sizes $L = 2, 3$ fm. The contributions coming from the Born term and from t_{00}^+ are plotted separately for both, the relativistic and the nonrelativistic Lüscher formula. The range of values covered by varying g from 0.18 to 0.79 in the relativistic formula is shaded in gray. Despite the large uncertainties the main message to be taken from the figures is that these FVC are negligibly small even for volumes as small as $L = 2$ fm.

We find it nonetheless instructive to discuss in some details some features which one can read off from the numerical analysis. First of all we remark that the deviation between the relativistic and the nonrelativistic result comes mainly from the t_{00}^+ term and it is very small compared to the uncertainty coming from the coupling constant. A detailed analysis of the size of the deviation will be given below.
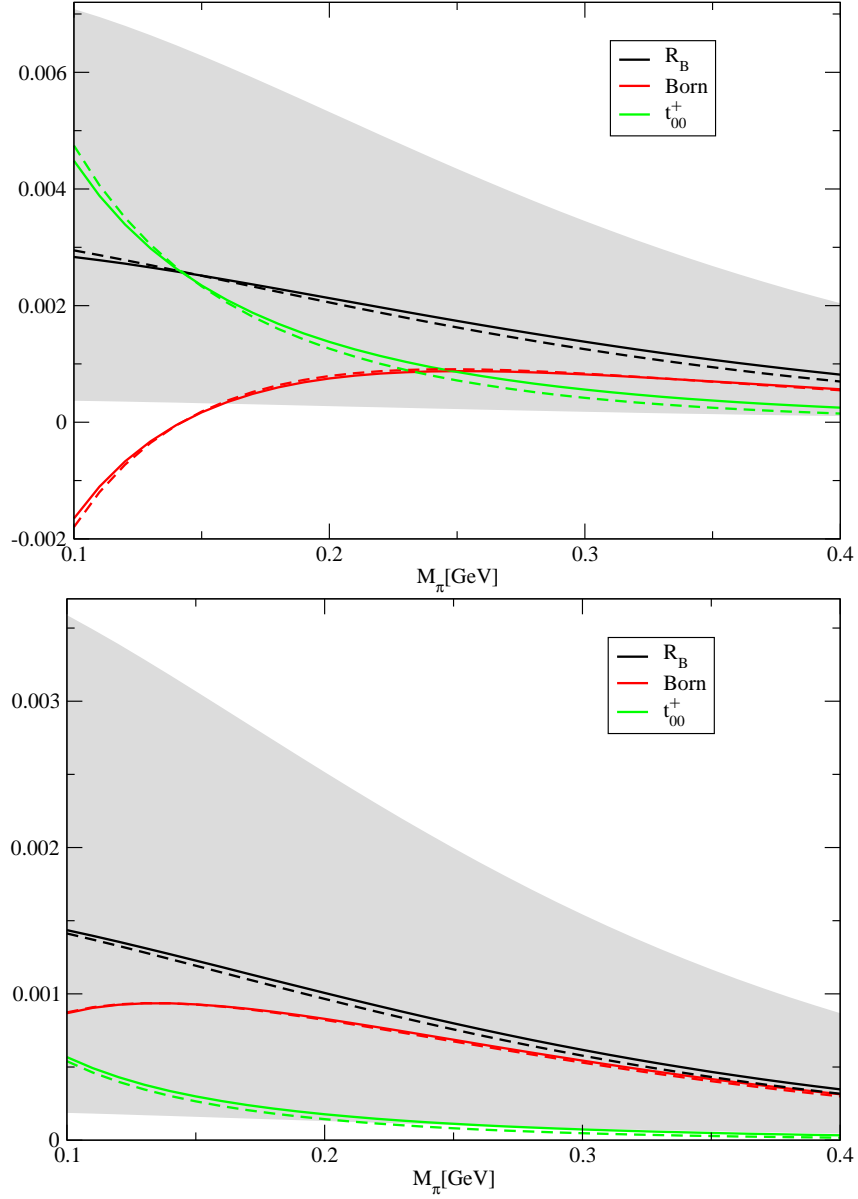
26

Figure 9: Finite volume effects as a function of the pion mass for a box size of $L = 2\,\mathrm{fm}$, in the upper panel for the D, in the lower panel for the B meson. The contributions of the different terms to the Lüscher formula are shown separately, the finite volume effect R_H is given by the sum. Solid lines are for the relativistic, dashed lines for the nonrelativistic formalism, the shaded area is the uncertainty on the relativistic result coming from the coupling constant g. Note that for $L = 2\,\mathrm{fm}$, the pion mass should fulfill $M_\pi \geq 0.2\,\mathrm{GeV}$ in order to stay in the region of validity of the Lüscher formula.
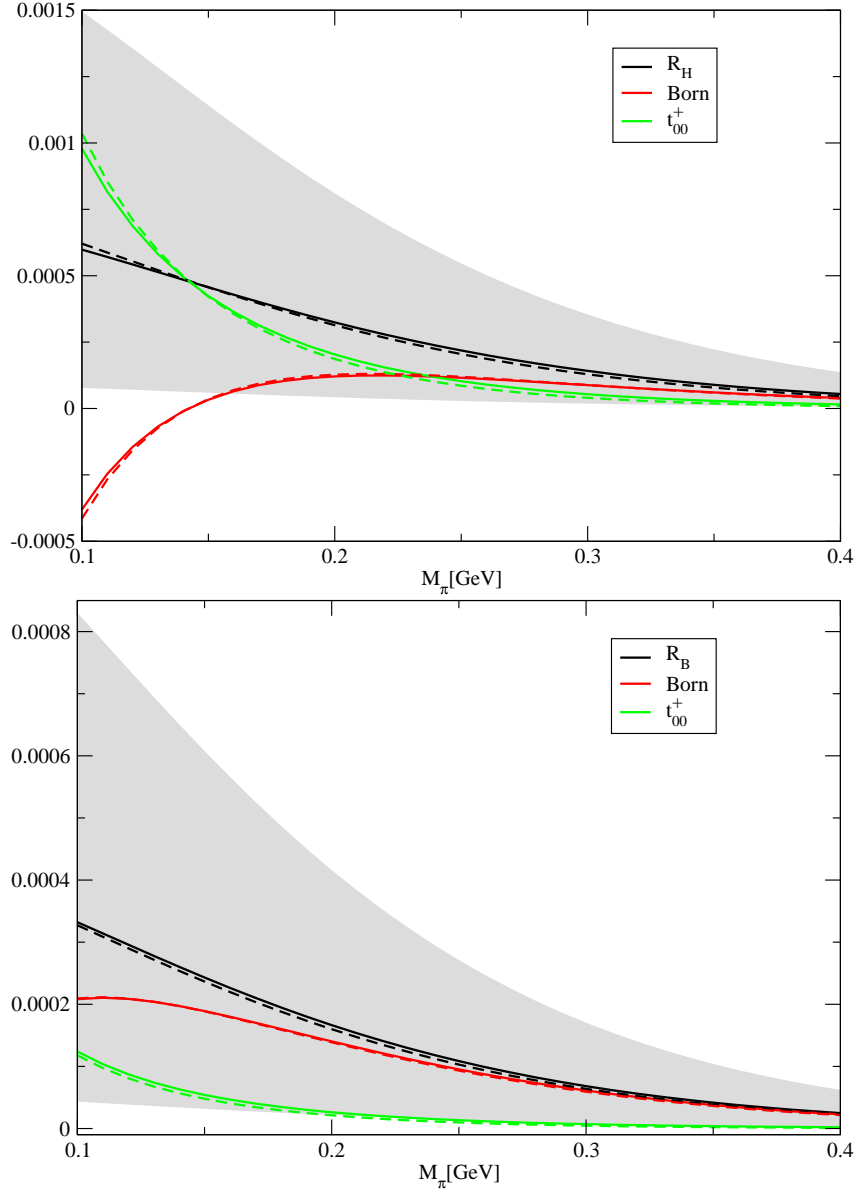
Figure 10: Finite volume effects as a function of the pion mass for a box size of $L = 3\,\text{fm}$: upper panel for the D, lower panel for the B meson. The contributions of the different terms to the Lüscher formula are shown separately, the finite volume effect R_H is given by the sum. Solid lines are for the relativistic, dashed lines for the nonrelativistic formalism, the shaded area is the uncertainty on the relativistic result coming from the coupling constant g. Note that for $L = 3\,\text{fm}$, the pion mass should fulfill $M_\pi \geq 0.13\,\text{GeV}$ in order to stay in the region of validity of the Lüscher formula.

For the B meson, the Born term compensates parts of the very large t_{00}^+ contribution at small pion masses, while for larger pion masses, both contributions are positive and of similar size. For the D meson the Born term clearly dominates the finite volume effect. The net effect is smaller for the heavier B meson and the t_{00}^+ contribution is reduced more than the Born term, as it is suppressed by an additional factor of $1/m_H$.

In order to compare the results from the relativistic and the nonrelativistic framework we define the relative difference between the two as

$$\delta_H = R_H^{\text{rel}}/R_H^{\text{nrel}} - 1 \; . \tag{44}$$

Numerical evaluation shows that δ_H indeed goes to zero for very large heavy meson masses. In the following, we give δ_H for physical values of the masses for a box size of $L = 3\,\text{fm}$. For the D meson with $m_D = 1.87\,\text{GeV}$ and $\Delta_* = 0.142\,\text{GeV}$ it is about 0.75%, for the B meson with $m_B = 5.28\,\text{GeV}$ and $\Delta_* = 0.046\,\text{GeV}$ about 2.5%. Because R_H is proportional to g^2, δ_H is independent of the coupling constant and consequently we do not give an error on these numbers. The absolute value of δ_H is very slowly decreasing with growing L such that the given values are good estimates for any box size. For unphysical pion masses, δ_H can become quite large, indicating that the nonrelativistic framework is not very well suited for large pion masses. For $M_\pi = 0.4\,\text{GeV}$, say, it is about 10% for the B and about 17% for the D meson.

Surprisingly, despite being the leading order term of a $1/m_H$ expansion, the nonrelativistic framework is more accurate for the lighter D meson. The reason is that δ_H also depends on the mass splitting Δ_*. If no heavy quark symmetry breaking effects are taken into account, i.e. when $\Delta_* = 0$, the agreement is better for the B meson.

We add some comments on the role of the step function in Eq. (34), which is nonzero if

$$\Delta_* < \tilde{\Delta}_* = \sqrt{m_H^2 + M_\pi^2} - m_H \approx \frac{M_\pi^2}{2m_H} \; . \tag{45}$$

By varying the parameter Δ_* between zero and the physical value observed for the case of the D and B mesons we can interpolate between the case in which the singularity structure of the amplitude is exactly like in the case of the nucleon (formally reached in the infinite quark mass limit), and the physical case with the H^* meson nondengenerate with the H meson. This corresponds to moving the pole in the ν-plane from the left-hand side to the right-hand side of the imaginary axis, as shown in Fig. 1. How this affects the FVC is demonstrated in Fig. 11, where the finite volume effect is plotted as a function of the mass splitting Δ_*. There one can clearly see the point
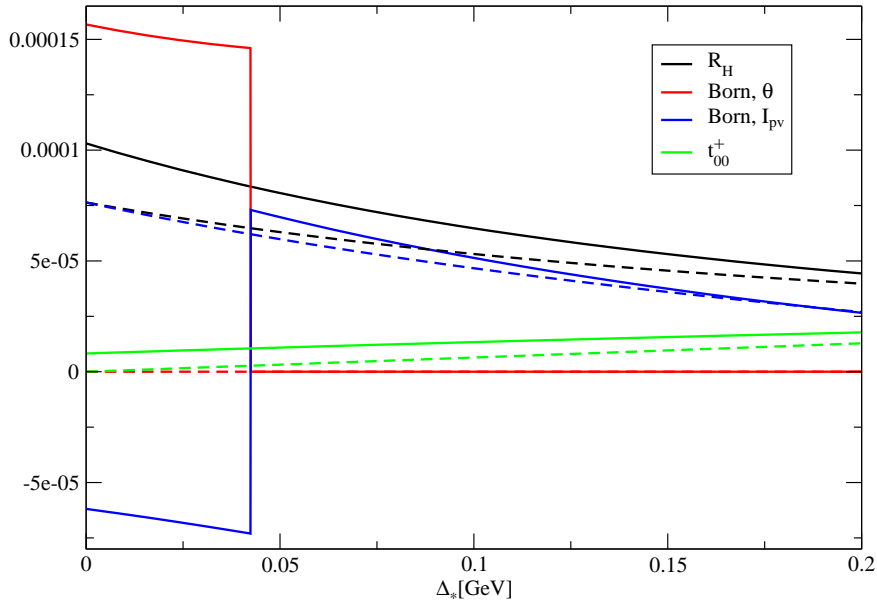
Figure 11: Finite volume effect for the D meson as a function of Δ_* with $L = 3\,\mathrm{fm}$ and $M_\pi = 0.4\,\mathrm{GeV}$. Solid lines are for the relativistic, dashed lines for the nonrelativistic formalism. The Born term has been split up in the contribution containing the step function and the one with the integral I_{pv}. The latter has a discontinuity, which is compensated by the former that starts to contribute exactly at this point. The error band has been omitted.

where the step function starts to contribute. At the same point, the other contribution to the Born term, containing the integral I_{pv} is discontinuous. This is due to the fact that $\bar{\varepsilon}_\pi$ goes through zero at $\Delta_* = \tilde{\Delta}_*$, while the product $\bar{\varepsilon}_\pi I_{\mathrm{pv}}$ goes to a nonzero value in the limit $\bar{\varepsilon}_\pi \to 0$ and I_{pv} is even in $\bar{\varepsilon}_\pi$. The term proportional to the step function compensates this effect such that the resulting finite volume effect is continuous. Indeed this term arises from a deformation of the integration path which keeps the pole due to H^* particle always to its right-hand side, even when the pole moves to the left-hand side of the imaginary axis. Since in this way the integration path does not cross any singularity as we change Δ^*, the integral remains analytic in Δ^* and we get a continuous curve. The figure also shows that in the nonrelativistic version of the Lüscher formula the mass shift is continuous even without the step function term, because $\tilde{\varepsilon}_\pi$ is always negative for $\Delta_* \geq 0$ and thus the point of the sign change is not in the range of validity of the Lüscher formula.

Other than for the nucleon, where the physical observables entering the Lüscher formula are best known at physical quark mass, the limited knowl-

30

edge on the coupling constant $g_{\pi HH^*}$ does not allow for a better accuracy on the FVC at the physical point in the case of the heavy meson. Also, it is very challenging to perform lattice simulations for heavy mesons with very small masses for the light quarks and thus we refrain from discussing this situation in detail.

7   Summary and conclusions

In this paper we have evaluated the finite volume corrections to the mass of nucleons and heavy mesons in the p-regime on the basis of the resummed Lüscher formula. The latter relates the finite size effect for the mass of a particle P to an integral over the forward πP scattering amplitude. We give simple analytic formulae which express the finite volume corrections to the nucleon and heavy meson masses in terms of only a handful of physical observables.

In the case of the nucleon, these observables are the pion mass M_π, the proton mass m_N, the pion–nucleon coupling constant $g_{\pi N}$ and the subthreshold parameters d_{i0}^+. Relying on the chiral representation of these quantities, one only needs to know the values of the chiral low-energy constants (LEC) to be able to predict the finite volume effects as a function of the quark mass. Fitting the nucleon mass m_N and the axial charge g_A to lattice results as well as fixing the other observables at the physical point, we extract values for these LEC. These values are then used as a basis for our numerical analysis which shows that:

- At the physical point, i.e. for a pion mass of $M_\pi = 0.140\,\text{GeV}$, the relative finite size effects drop below 1% for $L \geq 3.5\,\text{fm}$.

- At the physical point and box sizes of $L \geq 3\,\text{fm}$ we can predict the relative finite size effect with a precision of about 1‰.

- For unphysical pion masses, the relative finite size effects stay below 10%. However, moving away from the physical point, the precision deteriorates quickly and an accurate prediction of the finite size effect becomes impossible. For instance, in a box of the size $L = 2\,\text{fm}$ and for $M_\pi = 0.3\,\text{GeV}$, the relative finite size effect can be between 0% and 6%.

- The finite size effects strongly depend on the order p^2 LEC c_i and on the quark mass dependence of $g_{\pi N}$ (and therefore of g_A). Future analyses of better lattice data should exploit these relations to extract interesting information about these quantities.

- Our final results for the relative FVC are tabulated in Tab. 2.

We stress that it is thanks to the resummed Lüscher formula that one can relatively easily evaluate higher order contributions to the final volume effects and better assess the uncertainties. At the plain one-loop level in chiral perturbation theory [14], for example, the quark mass dependence of g_A does not yet play a role, and the contribution of the subthreshold coefficient d_{20}^+ is still absent. Both these effects are important, as we have shown, and substantially contribute to the uncertainties.

In the case of a heavy meson much less is known about the scattering amplitude of pions off them. At present, the best we could do is to analyze this at tree level in the heavy meson chiral perturbation theory approach. At this order, the amplitude can be expressed in terms of the pion mass M_π and the $B^{(*)}$ and $D^{(*)}$ meson masses as well as the coupling constant g describing the $\pi H H^*$ coupling (with $H = D$ or B). The numerical analysis is performed with these as input and shows that:

- The limited knowledge on the coupling constant g leads to large error bars in the numerical results. A higher order calculation of the finite volume effect is only worthwhile once this has improved.

- Despite our ignorance about the coupling constant g the FVC come out to be negligible (well below 1%) in all regions of the parameter space we have explored.

Although the practical interest of a calculation of the FVC for heavy mesons appears to be limited (in view of the fact that they are small), we found a detailed analysis of some of its features very instructive. We have discussed in particular the difference between a relativistic and a nonrelativistic version of Lüscher's formula and analyzed the dependence of the FVC on the size of the splitting between the pseudoscalar and the vector heavy meson.

Acknowledgments

$M_\pi[\mathrm{GeV}]$	$m_N[\mathrm{GeV}]$	$\delta_{m_N}[\mathrm{GeV}]$	Collaboration
0.13957	0.93827	0.00008	physical point
0.192	0.990	0.037	BMW
0.208	0.951	0.021	BMW
0.271	1.067	0.030	BMW
0.307	1.132	0.031	BMW
0.318	1.097	0.026	BMW
0.320	1.124	0.026	BMW

Table 3: Data points for the fit of the nucleon mass, taken from Ref. [1].

A   Low energy constants

The LEC c_i and d_{18} are scale independent. For the remaining LEC the scale independent combinations are given by

$$
\begin{aligned}
\bar{d}_{16} &= d_{16}^r(\mu) - \frac{g\,(4-g^2)}{8NF_\pi^2} \ln \frac{M_\pi}{\mu}, \\
\tilde{e}_1 &= e_1^r(\mu) - \frac{\frac{3}{2}g^2 - \frac{3}{2}(8c_1 - c_2 - 4c_3)m}{NF^2m} \ln \frac{M_\pi}{\mu} \\
\tilde{e}_3 &= e_3^r(\mu) + \frac{1 + 3g^2 + \frac{22}{3}g^4 + 8c_1 m + c_2 m - 4c_3 m}{NF^2m} \ln \frac{M_\pi}{\mu}, \\
\tilde{e}_4 &= e_4^r(\mu) - \frac{10 + 12g^2 + \frac{52}{3}g^4 + 8c_2 m}{NF^2m} \ln \frac{M_\pi}{\mu}, \\
\tilde{e}_6 &= e_6^r(\mu) + \frac{12 + 8g^2 + 8g^4}{NF^2m} \ln \frac{M_\pi}{\mu},
\end{aligned}
\tag{46}
$$

with $N = 16\pi^2$.

B   Details of the fits

The lattice results for the nucleon mass and the axial charge which are used in the fit are shown in Tab. 3 and 4. We intend not to strain the chiral expansions too much and do not include lattice results with pion masses significantly above 350 MeV. For the remaining quantities, only the value at the physical point, known from experiment [42], is available,

$$
\begin{aligned}
g_{\pi N} &= 13.39 \pm 0.08 \ , & M_\pi d_{00} &= -1.46 \pm 0.10 \ , \\
M_\pi^3 d_{10} &= 1.14 \pm 0.02 \ , & M_\pi^5 d_{20} &= 0.200 \pm 0.005 \ .
\end{aligned}
\tag{47}
$$

$M_\pi[\,\mathrm{GeV}]$	g_A	δ_{g_A}	Collaboration
0.13957	1.269	0.003	physical point
0.313	1.230	0.100	ETM
0.350	1.210	0.070	RBC/UKQCD
0.352	1.250	0.060	LHPC

Table 4: Data points for the fit of the axial charge. The data points are taken from Refs. [39–41]

.

The LEC $\bar\ell_i$ from the mesonic order p^4 Lagrangian are not determined in the fit, but are taken as input parameters without an error. We use the values given in Ref. [43]. For the pion decay constant F_π, the two-loop result from Ref. [44] with the values of the LEC as discussed in Ref. [10] is used. We use the standard χ^2 function

$$\chi^2 \;=\; \sum_{i,k} \left(\frac{y_k(\mathbf{x}, M_i) - \bar y_{k,i}}{\delta_{k,i}} \right)^2 \tag{48}$$

where $y_k(\mathbf{x}, M_i)$ is the chiral representation of quantity y_k evaluated at the pion mass M_i. The LEC are collected in the vector $\mathbf{x}$ and $\bar y_{k,i}$ denotes the data point of quantity y_k at the pion mass M_i with the error $\delta_{k,i}$. The error σ_{y_k} of the quantity y_k is given by

$$\sigma_{y_k}^2 = \frac{\partial y_k}{\partial x_l} \frac{\partial y_k}{\partial x_m} C_{lm} \tag{49}$$

with $\mathbf{C}$ the correlation matrix of the LEC.

C   Formalism of heavy meson χPT

At present there are two frameworks to include heavy mesons into chiral perturbation theory: a relativistic one introduced in Ref. [30] and a nonrelativistic one introduced in Ref. [31]. We only present the two Lagrangians very briefly; for a detailed discussion, we refer to the original publications and to Refs. [45, 46]. All conventions we use have been adapted to agree with the latter. We give the relativistic Lagrangian for fields $B_a^{(Q)}$ and $B_a^{*(Q)}$ that annihilate a pseudoscalar and a vector meson consisting, respectively, of a heavy quark Q and a light antiquark q_a. From these we build the field

$$\mathcal{B}_a = \left(\frac{i\not{D}_{ab} + m_H \delta_{ab}}{2m_H} \right) [iB_b\gamma_5 + B_b^{*\mu}\gamma_\mu], \qquad \bar{\mathcal{B}}_a = \gamma^0 \mathcal{B}_a^\dagger \gamma^0, \tag{50}$$

where we omitted the superscript for simplicity. The covariant derivative is given by $D^\mu_{ab} = \partial^\mu \delta_{ab} - \Gamma^\mu_{ba}$, with the connection

$$\Gamma_\mu = \frac{1}{2}[u^\dagger, \partial_\mu u] = \frac{1}{2}(u^\dagger \partial_\mu u + u \partial_\mu u^\dagger) = \frac{i}{4F^2} \varepsilon^{abc} \tau^a \pi^b \partial_\mu \pi^c + \mathcal{O}(\pi^4). \quad (51)$$

We also need the vielbein

$$u_\mu = i\{u^\dagger, \partial_\mu u\} = i(u^\dagger \partial_\mu u - u \partial_\mu u^\dagger) = -\frac{1}{F}\tau^a \partial_\mu \pi^a + \mathcal{O}(\pi^3). \quad (52)$$

From these building blocks we can construct the relativistic heavy meson Lagrangian, which is

$$\mathcal{L}_{HM,\ rel} = -m_H \operatorname{Tr}\left[\bar{\mathcal{B}}_a(i\not{D}_{ab} - m_H \delta_{ab})\mathcal{B}_b - \frac{g}{2}\bar{\mathcal{B}}_a \mathcal{B}_b \gamma_\mu \gamma_5 u^\mu\right]. \quad (53)$$

The second term is not contained in the Lagrangian of Ref. [30] and had to be added here as it is the source of the one-loop self-energy contributions.

By means of a nonrelativistic decomposition procedure similar to the one used in heavy baryon chiral perturbation theory [47, 48], we can derive the Lagrangian of Ref. [31] from this. Instead of $\mathcal{B}_a$, we use the field

$$H_a = \frac{\not{v}+1}{2}[iP_a \gamma_5 + P^{*\mu}_a \gamma_\mu], \quad \bar{H}_a = \gamma^0 H^\dagger_a \gamma^0 = [iP^\dagger_a \gamma_5 + P^{*\mu\dagger}_a \gamma_\mu]\frac{\not{v}+1}{2}, \quad (54)$$

where v^μ is the four velocity of the heavy meson and the fields P_a and $P^{*\mu}_a$ replace B_a and $B^{*\mu}_a$ respectively. Note that they differ in normalization by a factor $1/\sqrt{m_H}$, which ensures that the nonrelativistic Lagrangian does not depend on m_H. Inserting these fields into Eq. (53) and expanding to leading order in $1/m_H$, we find the nonrelativistic Lagrangian

$$\mathcal{L}_{HM,\ nrel} = -i \operatorname{Tr}\left(\bar{H}_a v_\mu \partial^\mu H_a\right)$$
$$+ i \operatorname{Tr}\left(\bar{H}_a H_b v_\mu \Gamma^\mu_{ba}\right) + \frac{g}{2} \operatorname{Tr}\left(\bar{H}_a H_b \gamma_\mu \gamma_5 u^\mu_{ba}\right). \quad (55)$$

Up to the phase conventions, this agrees with the nonrelativistic Lagrangian of Ref. [31].

References

[1] S. Durr *et al.*, Science **322** (2008) 1224 [arXiv:0906.3599 [hep-lat]].

[2] S. Aoki *et al.* [PACS-CS Collaboration], Phys. Rev. D **79** (2009) 034503 [arXiv:0807.1661 [hep-lat]].

[3] S. Weinberg, Physica A **96** (1979) 327.

[4] J. Gasser and H. Leutwyler, Annals Phys. **158** (1984) 142.

[5] J. Gasser and H. Leutwyler, Nucl. Phys. B **250** (1985) 465.

[6] J. Gasser and H. Leutwyler, Phys. Lett. B **184** (1987) 83.

[7] J. Gasser and H. Leutwyler, Nucl. Phys. B **307** (1988) 763.

[8] M. Lüscher, DESY 83/116, *Lecture given at Cargese Summer Inst., Cargese, France, Sep 1-15, 1983.*

[9] M. Lüscher, Commun. Math. Phys. **104** (1986) 177.

[10] G. Colangelo and S. Durr, Eur. Phys. J. C **33** (2004) 543 [arXiv:hep-lat/0311023].

[11] G. Colangelo and C. Haefeli, Phys. Lett. B **590** (2004) 258 [arXiv:hep-lat/0403025].

[12] G. Colangelo, S. Durr and C. Haefeli, Nucl. Phys. B **721** (2005) 136 [arXiv:hep-lat/0503014].

[13] G. Colangelo, U. Wenger and J. M. S. Wu, arXiv:1003.0847 [hep-lat].

[14] A. Ali Khan *et al.* [QCDSF-UKQCD Collaboration], Nucl. Phys. B **689** (2004) 175 [hep-lat/0312030].

[15] Y. Koma and M. Koma, Nucl. Phys. B **713** (2005) 575 [arXiv:hep-lat/0406034].

[16] G. Colangelo, A. Fuhrer and C. Haefeli, Nucl. Phys. Proc. Suppl. **153** (2006) 41 [arXiv:hep-lat/0512002].

[17] G. Colangelo and C. Haefeli, Nucl. Phys. B **744** (2006) 14 [arXiv:hep-lat/0602017].

[18] J. L. Goity, Phys. Lett. B **249** (1990) 495.

[19] D. Arndt and C. J. D. Lin, Phys. Rev. D **70** (2004) 014503 [arXiv:hep-lat/0403012].

[20] C. J. D. Lin, Nucl. Phys. Proc. Suppl. **140** (2005) 494 [arXiv:hep-lat/0409076].

[21] F. Bernardoni, P. Hernandez and S. Necco, [arXiv:0910.2537 [hep-lat]].

[22] F. Bernardoni, P. Hernandez and S. Necco, [arXiv:0910.2630 [hep-lat]].

[23] T. Becher and H. Leutwyler, JHEP **0106** (2001) 017 [arXiv:hep-ph/0103263].

[24] T. Becher and H. Leutwyler, Eur. Phys. J. C **9** (1999) 643 [arXiv:hep-ph/9901384].

[25] V. Bernard and U. G. Meissner, Phys. Lett. B **639** (2006) 278 [arXiv:hep-lat/0605010].

[26] J. Gasser, V. E. Lyubovitskij and A. Rusetsky, Phys. Rept. **456** (2008) 167 [arXiv:0711.3522 [hep-ph]].

[27] N. Fettes, V. Bernard and U. G. Meissner, Nucl. Phys. A **669** (2000) 269 [arXiv:hep-ph/9907276].

[28] N. Fettes, U. G. Meissner and S. Steininger, Nucl. Phys. A **640** (1998) 199 [arXiv:hep-ph/9803266].

[29] M. Procura, B. U. Musch, T. Wollenweber, T. R. Hemmert and W. Weise, Phys. Rev. D **73** (2006) 114510 [arXiv:hep-lat/0603001].

[30] G. Burdman and J. F. Donoghue, Phys. Lett. B **280** (1992) 287.

[31] M. B. Wise, Phys. Rev. D **45** (1992) 2188.

[32] A. Khodjamirian, R. Ruckl, S. Weinzierl and O. I. Yakovlev, Phys. Lett. B **457** (1999) 245 [arXiv:hep-ph/9903421].

[33] A. Anastassov *et al.* [CLEO Collaboration], Phys. Rev. D **65** (2002) 032003 [arXiv:hep-ex/0108043].

[34] A. Abada *et al.*, Phys. Rev. D **66** (2002) 074504 [arXiv:hep-ph/0206237].

[35] A. Abada *et al.*, Nucl. Phys. Proc. Suppl. **119** (2003) 641 [arXiv:hep-lat/0209092].

[36] A. Abada, D. Becirevic, P. Boucaud, G. Herdoiza, J. P. Leroy, A. Le Yaouanc and O. Pene, JHEP **0402** (2004) 016 [arXiv:hep-lat/0310050].

[37] D. Becirevic, B. Blossier, P. Boucaud, J. P. Leroy, A. LeYaouanc and O. Pene, PoS **LAT2005** (2006) 212 [arXiv:hep-lat/0510017].

[38] D. Becirevic, B. Blossier, E. Chang and B. Haas, Phys. Lett. B **679** (2009) 231 [arXiv:0905.3355 [hep-ph]].

[39] R. Baron *et al.* [ETM Collaboration], PoS **LATTICE2008** (2008) 162.

[40] T. Yamazaki *et al.* [RBC+UKQCD Collaboration], Phys. Rev. Lett. **100** (2008) 171602 [arXiv:0801.4016 [hep-lat]].

[41] D. B. Renner *et al.* [LHPC Collaboration], J. Phys. Conf. Ser. **46** (2006) 152 [arXiv:hep-lat/0607008].

[42] G. Höhler, in Landolt-Börnstein, 9b2, ed. H. Schopper (Springer, Berlin, 1983).

[43] G. Colangelo, J. Gasser and H. Leutwyler, Nucl. Phys. B **603** (2001) 125 [arXiv:hep-ph/0103088].

[44] J. Bijnens, G. Colangelo and P. Talavera, JHEP **9805** (1998) 014 [arXiv:hep-ph/9805389].

[45] H. Georgi, *Heavy quark effective field theory* in *Perspectives in the standard model. Proceedings*, Theoretical Advanced Study Institute in Elementary Particle Physics, Boulder, USA, June 2-28, 1991.

[46] A. V. Manohar and M. B. Wise, Camb. Monogr. Part. Phys. Nucl. Phys. Cosmol. **10** (2000) 1.

[47] E. E. Jenkins and A. V. Manohar, Phys. Lett. B **255** (1991) 558.

[48] V. Bernard, N. Kaiser, J. Kambor and U. G. Meissner, Nucl. Phys. B **388** (1992) 315